Research Paper

NOX4-mediated ROS production induces apoptotic cell death via down-regulation of c-FLIP and Mcl-1 expression in combined treatment with thioridazine and curcumin

Seung Un Seo[a],[1], Tae Hwan Kim[b],[1], Dong Eun Kim[b], Kyoung-jin Min[a],*, Taeg Kyu Kwon[a],*

[a] Department of Immunology, School of Medicine, Keimyung University, 2800 Dalgubeoldaero, Dalseo-Gu, Daegu 704-701, South Korea
[b] Department of Otolaryngology, School of Medicine, Keimyung University, 2800 Dalgubeoldaero, Dalseo-Gu, Daegu 704-701, South Korea

ARTICLE INFO

ABSTRACT

Thioridazine is known to have anti-tumor effects by inhibiting PI3K/Akt signaling, which is an important signaling pathway in cell survival. However, thioridazine alone does not induce apoptosis in head and neck squamous cell carcinoma (AMC-HN4), human breast carcinoma (MDA-MB231), and human glioma (U87MG) cells. Therefore, we investigated whether combined treatment with thioridazine and curcumin induces apoptosis. Combined treatment with thioridazine and curcumin markedly induced apoptosis in cancer cells without inducing apoptosis in human normal mesangial cells and human normal umbilical vein cells (EA.hy926). We found that combined treatment with thioridazine and curcumin had synergistic effects in AMC-HN4 cells. Among apoptosis-related proteins, thioridazine plus curcumin induced down-regulation of c-FLIP and Mcl-1 expression at the post-translational levels in a proteasome-dependent manner. Augmentation of proteasome activity was related to the up-regulation of proteasome subunit alpha 5 (PSMA5) expression in curcumin plus thioridazine-treated cells. Combined treatment with curcumin and thioridazine produced intracellular ROS in a NOX4-dependent manner, and ROS-mediated activation of Nrf2/ARE signaling played a critical role in the up-regulation of PSMA5 expression. Furthermore, ectopic expression of c-FLIP and Mcl-1 inhibited apoptosis in thioridazine and curcumin-treated cells. Therefore, we demonstrated that thioridazine plus curcumin induces proteasome activity by up-regulating PSMA5 expression via NOX4-mediated ROS production and that down-regulation of c-FLIP and Mcl-1 expression post-translationally is involved in apoptosis.

1. Introduction

Thioridazine (10-[2-(1-methyl-2-piperidyl) ethyl]-2-(methylthio) phenothiazine) is an anti-psychotic drug for treating psychosis and schizophrenia [1,2]. Recently, anti-cancer effects of thioridazine have been reported. Thioridazine induces apoptosis [3–8] as well as inhibits angiogenesis [9,10] and metastasis [11] in cancer cells. Furthermore, thioridazine induced stem cell differentiation to overcome neoplastic self-renewal [12] as well as inhibited sphere formation of stem cells and decreased the stemness [13]. Several molecular mechanisms of anti-cancer effects of thioridazine have been known. Inhibition of PI3K/Akt and mTOR signaling are involved in thioridazine-induced apoptosis [3]. Tousled-like kinases (TLKs), which are involved in chromatin assembly and DNA repair, are also inhibited by thioridazine, resulting in potentiation of tumor killing effects [14]. In addition, thioridazine inhibits

breast cancer cell proliferation via calmodulin antagonism [15]. Instead of single thioridazine treatment, combined treatment with thioridazine and anti-cancer drugs can improve the therapeutic effect and reduce side effects. For example, a sub-toxic dosage of thioridazine plus tumor necrosis factor-related apoptosis-inducing ligand (TRAIL) induced apoptosis in renal carcinoma Caki cells through the production of reactive oxygen species (ROS) [16]. Combined treatment with thioridazine and doxorubicin maximizes the anti-cancer effect in breast cancer cells [17,18].

For cancer treatment and prevention, natural compounds extracted from plants or released by microbes are used. Curcumin is one cancer chemopreventive compound; it is a polyphenolic phytochemical extracted from the rhizomes of the *Curcuma longa* plant. Curcumin could induce apoptosis in cancer cells [19–24] as well as inhibit VEGF and osteopontin-induced angiogenesis [25,26]. Furthermore, curcumin

inhibits H_2O_2-induced invasion of pancreatic cancer [27] and blocks invasion of ovarian cancer spheroids into the mesothelial monolayers [28]. In addition, many groups have reported that curcumin enhances TRAIL-, 5-fluorouracil-, gemcitabine- and irradiation-induced cell death [29–35].

In the present study, we assessed the effect of combined treatment with thioridazine and curcumin on apoptosis and investigated the mechanism of anti-cancer effects of thioridazine plus curcumin in human head and neck cancer AMC-HN4 cells.

2. Materials and methods

2.1. Cells and materials

Human head and neck cancer AMC-HN4 cells were obtained from Asan Medical Center. MDA-MB-231, U87MG, and EA.hy926 cells were purchased from the American Type Culture Collection (Manassas, VA, USA). Primary cultures of human mesangial cells (Cryo NHMC) were purchased from Clonetics (San Diego, CA). The cells were cultured in Dulbecco's modified Eagle's medium that contained 10% fetal bovine serum, 20 mM Hepes buffer, and 100 µg/ml gentamicin. The PCR primers were purchased from Macrogen Inc. (Seoul, Korea), and other chemicals were purchased from Sigma (St. Louis, MO). Sulforaphane, N-acetyl-L-cysteine (NAC) and Trolox were obtained from Calbiochem (San Diego, CA). Anti-Bcl2, anti-Bcl-xL, anti-Mcl-1, anti-XIAP, anti-Nrf2, and anti-PARP antibodies were purchased from Santa Cruz Biotechnology (Santa Cruz, CA). Anti-cleaved caspase-3 and anti-cIAP1 antibodies were obtained from Cell Signaling Technology (Beverly, MA). Anti-caspase 3, anti-c-FLIP antibody was obtained from ALEXIS Corporation (San Diego, CA). Anti-PSMA5 antibodies were purchased from Cell Signaling Technology (Beverly, MA). Anti-peroxiredoxin-SO₃ antibody was purchased from AbFRONTIER (Seoul, Korea). Anti-Nox4 was obtained from Abcam (Cambridge, MA). Anti-actin antibody was obtained from Sigma (St. Louis, MO). The human Mcl-1 and c-FLIP expression vector was constructed, as described previously [36,37].

2.2. Flow cytometry analysis

For flow cytometry, the cells were resuspended in 100 µl of phosphate-buffered saline (PBS), and 200 µl of 95% ethanol was added while the cells were being vortexed. Then, the cells were incubated at 4 °C for 1 h, washed with PBS, resuspended in 250 µl of 1.12% sodium citrate buffer (pH 8.4) and 12.5 µg of RNase and incubated for an additional 30 min at 37 °C. The cellular DNA was then stained by adding 250 µl of a propidium iodide solution (50 µg/ml) to the cells for 30 min at room temperature. The stained cells were analyzed by fluorescent-activated cell sorting on a FACScan flow cytometer to determine the relative DNA content, which was based on the red fluorescence intensity.

2.3. Western blot analysis

For the Western blot experiments, the cells were washed with cold PBS and lysed on ice in modified RIPA buffer (50 mM Tris-HCl pH 7.4, 1% NP-40, 0.25% Na-deoxycholate, 150 mM NaCl, 1 mM Na_3VO_4, and 1 mM NaF) containing protease inhibitors (100 µM phenylmethylsulfonyl fluoride, 10 µg/ml leupeptin, 10 µg/ml pepstatin, and 2 mM EDTA). The lysates were centrifuged at 10,000*g* for 10 min at 4 °C, and the supernatant fractions were collected. The proteins were separated by SDS-PAGE electrophoresis and transferred to Immobilon-P membranes. The specific proteins were detected using an enhanced chemiluminescence (ECL) Western blot kit according to the manufacturer's instructions.

2.4. Determination of synergy and cell viability assay

The possible synergistic effect of thioridazine and curcumin was evaluated using the isobologram method. In brief, the cells were treated with different concentrations of thioridazine and curcumin alone or in combination. After 24 h, the XTT assay was employed to measure the cell viability using a WelCount Cell Viability Assay Kit (WelGENE, Daegu, Korea). Reagent was added to each well and each well was then measured with a multi-well plate reader (at 450 nm/690 nm). Relative survival was assessed and the concentration effect curves were used to determine the IC_{50} (the half-maximal inhibitory concentration) values for each drug alone and in combination with a fixed concentration of the second agent [38].

2.5. 4′,6′-Diamidino-2-phenylindole staining (DAPI) for nuclei condensation and fragmentation

AMC-HN4 cells were seeded at a density of 0.2×10^6 cells/well in 12-well plates and then attached overnight. Medium was replaced with fresh DMEM media, cells were treated with 10 µM thioridazine in the presence or absence of 0.5 µM curcumin for 24 h. To examine cellular nuclei, the cells were fixed with 1% paraformaldehyde on glass slides for 30 min at room temperature. After fixation, the cells were washed with PBS and a 300 nM 4′,6′-diamidino-2-phenylindole solution (Roche, Mannheim, Germany) was added to the fixed cells for 5 min. After the nuclei were stained, the cells were examined by fluorescence microscopy.

2.6. The DNA fragmentation assay

AMC-HN4 cells were seeded at a density of 0.2×10^6 cells/well in 12-well plates and then attached overnight. Cells were treated with 10 µM thioridazine in the presence or absence of 0.5 µM curcumin for 24 h. The cell death detection ELISA plus kit (Boerhringer Mannheim; Indianapolis, IN) was used to determine the level of apoptosis by detecting fragmented DNA within the nuclei of thioridazine-treated cells, curcumin-treated cells, or cells that had been treated with a combination of thioridazine and curcumin. Briefly, each culture plate was centrifuged for 10 min at 200*g*, the supernatant was removed, and the cell pellet was lysed for 30 min. Then, the plate was centrifuged again at 200*g* for 10 min, and the supernatant that contained the cytoplasmic histone-associated DNA fragments was collected and incubated with an immobilized anti-histone antibody. The reaction products were incubated with a peroxidase substrate for 5 min and measured by spectrophotometry at 405 and 490 nm (reference wavelength) with a microplate reader. The signals in the wells containing substrate alone were subtracted as the background.

2.7. Asp-Glu-Val-Asp-ase (DEVDase) activity assay

To evaluate DEVDase activity, cell lysates were prepared after their respective treatments with curcumin in the presence or absence of thioridazine. Assays were performed in 96-well microtiter plates by incubating 20 µg of cell lysates in 100 µl of reaction buffer (1% NP-40, 20 mM Tris-HCl, pH 7.5, 137 mM NaCl, 10% glycerol) containing a caspase substrate [Asp-Glu-Val-Asp-chromophore-p-nitroanilide (DVAD-pNA)] at 5 µM. Lysates were incubated at 37 °C for 2 h. Thereafter, the absorbance at 405 nm was measured with a spectrophotometer.

2.8. Reverse transcription polymerase chain reaction (RT-PCR)

Total RNA was isolated using the TriZol reagent (Life Technologies; Gaithersburg, MD), and the cDNA was prepared using M-MLV reverse transcriptase (Gibco-BRL; Gaithersburg, MD) according to the manufacturer's instructions [39,40]. The following primers were used for the

amplification of human c-FLIP, Mcl-1, PSMA5, and actin: c-FLIP (sense) 5′- CGG ACT ATA GAG TGC TGA TGG -3′ and (antisense) 5′- GAT TAT CAG GCA GAT TCC TAG -3′, Mcl-1 (sense) 5′- GCG ACT GGC AAA GCT TGG CCT CAA-3′ and (antisense) 5′- GTT ACA GCT TGG ATC CCA ACT GCA-3′, PSMA5 (sense) 5′- CTT GCA AGA AGT TTA TCA CAA GTC T -3′ and (antisense) 5′- GAA ATT CTG GCC AGG CTG C -3′, and actin (sense) 5′- GGC ATC GTC ACC AAC TGG GAC -3′ and (anti-sense) 5′- CGA TTT CCC GCT CGG CCG TGG -3′. The PCR amplification was performed using the following cycling conditions: 94 °C for 3 min followed by 17 (actin) or 23 cycles (c-FLIP, and Mcl-1, and PSMA5) of 94 °C for 45 s, 58 °C for 45 s, 72 °C for 1 min, and a final extension at 72 °C for 10 min. The amplified products were separated by electrophoresis on a 1.5% agarose gel and detected under UV light.

2.9. Proteasome activity assay

AMC-HN4 cells were seeded at a density of 0.2×10^6 cells/well in 12-well plates and then attached overnight. Cells were treated with 10 µM thioridazine plus 0.5 µM curcumin for 24 h. After treatment, chymotryptic proteasome activities were measured with Suc-LLVY-AMC (chymotryptic substrate, Biomol International, Plymouth Meeting, PA). Cells were collected, washed with PBS and lysed. A mixture containing 1 µg of cell lysate protein in 100 mM Tris-HCl (pH 8.0), 10 mM $MgCl_2$, and 2 mM ATP was incubated at 37 °C for 30 min with 50 µM Suc-LLVY-AMC. Enzyme activity was measured with a fluorometric plate reader at an excitation wavelength of 380 nm and an emission wavelength of 440 nm.

2.10. DNA transfection and luciferase assay

Transient transfection was performed in 6-well plates. One day before the transfection, AMC-HN4 cells were plated at approximately 60 to 80% confluence. The PSMA5/-277-Luc or ARE-Luc plasmid was transfected into the cells using Lipofectamine™ 2000 (Invitrogen, Carlsbad, CA, USA). After transfection, cells were treated with 10 µM thioridazine plus 0.5 µM curcumin or 200 µM sulforaphane for 24 h. To assess the promoter-driven expression of the luciferase gene, the cells were collected and disrupted by sonication in lysis buffer (25 mM Tris-phosphate, pH 7.8, 2 mM EDTA, 1% Triton X-100%, and 10% glycerol), and aliquots of the supernatant were used to analyze the luciferase activity according to the manufacturer's instructions (Promega, Madison, WI, USA).

2.11. Preparation of cytosol and nuclear extracts

AMC-HN4 cells were seeded at a density of 0.4×10^6 cells/well in 6-well plates and then attached overnight. Cells were pretreated with 5 mM NAC, 2 mM GEE, and 200 µM trolox for 30 min, and they were then treated with 10 µM thioridazine plus 0.5 µM curcumin for 24 h or treated with 10 µM thioridazine plus 0.5 µM curcumin for 1, 3, and 6 h. Following the required treatments, AMC-HN4 cells were trypsinized and suspended in buffer A (10 mM HEPES at pH 7.9, 10 mM KCl, 0.1 mM EDTA, 0.1 mM EGTA, 1 mM DTT, and 0.5 mM PMSF). After incubation on ice for 30 min, cells were centrifuged at 2500 rpm for 3 min to obtain a nuclear pellet. Supernatant fractions were collected as the cytosol extract. Buffer C (20 mM HEPES at pH 7.9, 0.4 M NaCl, 1 mM EDTA, 1 mM DTT, and 1 mM PMSF) was added, which was followed by rotation for 30 min at 4 °C. The resulting lysates were centrifuged at 12,000 rpm at 4 °C for 5 min. Supernatant fractions were collected as the nuclear extract

2.12. Small interfering RNAs

The GFP (control), Nrf2, PSMA5, and NOX4 small interfering RNA (siRNA) duplexes used in this study were purchased from Santa Cruz Biotechnology (Santa Cruz, CA, USA). Cells were transfected with siRNA using Oligofectamine Reagent (Invitrogen, Carlsbad, California, USA) according to the manufacturer's recommendations.

2.13. Measurement of reactive oxygen species (ROS)

Intracellular accumulation of ROS was determined using the fluorescent probes 2′, 7′-dichlorodihydrofluorescein diacetate (H_2DCFDA) and Mitosox Red. AMC-HN4 cells were treated with thioridazine and curcumin; then, cells were stained with the H_2DCFDA fluorescent dye or Mitosox Red for an additional 10 min. Afterwards, cells were trypsinized and resuspended in PBS, and fluorescence was measured at specific time intervals with a flow cytometer (Becton–Dickinson; Franklin Lakes, NJ, USA) or fluorescence microscope (Zeiss, Jena, Germany).

2.14. Detection of NBT (nitro blue tetrazolium)

AMC-HN4 cells were transiently transfected with a control siRNA or NOX4 siRNA. Twenty-four hours after transfection, cells were treated with 10 µM thioridazine plus 0.5 µM curcumin or 75 nM PMA for 12 h. After treatment, cells were washed twice in HBSS and incubated with NBT (1.6 mg/ml) in HBSS at 37 °C for 1 h. After fixation in 100% methanol and a wash in methanol, the formazan precipitates were dissolved by 560 µl 2 M KOH and 480 µl DMSO. The amount of reduced NBT was quantified by determination of the absorbance at 570 nm.

2.15. Measurement of hydrogen peroxide production

Hydrogen peroxide was determined using reaction mixture [100 µM Amplex Red and 0.2 U/ml HRP in Krebs–Ringer phosphate (KRPG) buffer (145 mM NaCl, 5.7 mM sodium phosphate, 4.86 mM KCl, 0.54 mM CaCl2, 1.22 mM MgSO4, 5.5 mM glucose, pH 7.35)]. AMC-HN4 cells were treated with 10 µM thioridazine in the presence or absence of 0.5 µM curcumin for 6 h, and then 50 µl media incubated with 50 µl of reaction mixture (100 µM Amplex Red and 0.2 U/ml HRP) for 10 min at 37 °C. The levels of hydrogen peroxide in the medium was detected by fluorescence of the oxidized Amplex Red product using excitation and emission wavelengths of 560 and 590 nm, respectively. Intracellular levels of H_2O_2 in cytoplasm were measured using the genetically encoded fluorescent sensors HyPer-Cyto (Evrogen, Moscow, Russia). In brief, AMC-HN4 cells were transiently transfected with HyPer-Cyto plasmids. After transfection, cells were treated with 10 µM thioridazine in the presence or absence of 0.5 µM curcumin. After 6 h, the cells were resuspended in 100 µl of phosphate-buffered saline (PBS), and HyPer fluorescence was detected by FACScan flow cytometer.

2.16. Measurement of glutathione

Glutathione (GSH) and glutathione disulfide (GSSG) was determined by a modification of the method, as previously described [41]. Cells were cultured in six-well plates and were lysed by 200 µl of lysis buffer (50 mM Tris–HCl, 1 mM EGTA, 1% Triton X-100). The cell lysate was deproteinized with the same volume of 10% 5-sulfosalicyclin acid. After centrifugation at 5000 g for 5 min at 4 °C, the supernatant was divided into 2 samples, 1 for GSH and 1 for GSSG measures. The amount of total GSH was determined by formation of 5-thio-2-nitrobenzoic acid (TBA) converted from 5,5-dithiobis(2-nitrobenzoic acid) (DTNB) [42]. GSSG was measured by the DTNB-GSSG reductase recycling assay after treating GSH with 2-vinylpyridine for 1 h at room temperature [43]. Total glutathione and GSSG levels were defined as the change in OD at 405 nm for 5 min at room temperature.

2.17. Statistical analysis

The data were analyzed using a one-way ANOVA and post-hoc comparisons (Student-Newman-Keuls) using the Statistical Package for
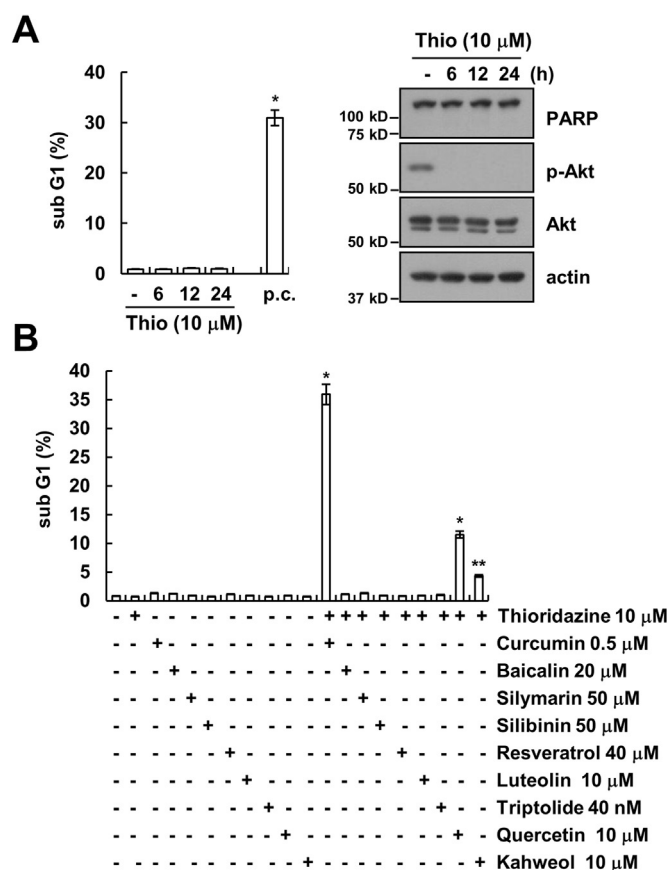
A

B

Fig. 1. The effect of thioridazine and combined treatment with thioridazine and natural compounds on apoptosis in human head and neck squamous cell carcinoma (AMC-HN4). (A) AMC-HN4 cells were with 10 µM thioridazine or 10 µM thioridazine plus 0.5 µM curcumin (p.c.: positive control; 24 h) for the indicated time periods. The sub-G1 fraction was measured by flow cytometry. The protein expression levels of PARP, phospho(p)-Akt, Akt and actin were determined by Western blot. The level of actin was used as a loading control. (B) AMC-HN4 cells were with the indicated concentrations of curcumin, baicalin, silymarin, silibinin, resveratrol, luteolin, triptolide, quercetin, and kahweol in the presence or absence of 10 µM thioridazine for 24 h. The sub-G1 fraction was measured by flow cytometry. The values in A and B represent the mean ± SD from three independent samples. * $p < 0.01$ compared to control. ** $p < 0.05$ compared to control.

Social Sciences 22.0 software (SPSS Inc.; Chicago, IL, USA).

3. Results

3.1. Combined treatment with thioridazine and curcumin induces apoptosis in cancer cells

Thioridazine has anti-cancer effects through inhibiting the PI3K/Akt signaling pathways. However, although thioridazine inhibits phosphorylation of Akt, cell death was not induced (Fig. 1A). Therefore, we examined whether combined treatment with natural compounds and thioridazine induces cell death. Among natural compounds, curcumin markedly induced apoptosis in thioridazine-treated cells (Fig. 1B). In addition, given curcumin sensitizes anti-cancer drugs-induced apoptosis [29–35], and we investigated whether combined treatment with thioridazine and curcumin induces cell death in cancer cells. As shown in Fig. 2A–C, combined treatment with thioridazine and curcumin induced apoptosis and PARP cleavage, which is a one of the apoptosis markers, in head and neck squamous cell carcinoma (AMC-HN4), human breast carcinoma (MDA-MB231), and human glioma (U87MG) cells. In contrast, thioridazine plus curcumin did not induce a morphological change or apoptosis in normal human mesangial cells (MC) and normal human umbilical vein cells (EA.hy926) (Fig. 2D).

Therefore, combined treatment with thioridazine and curcumin induces apoptosis in cancer cells without inducing apoptosis in normal cells.

3.2. Thioridazine plus curcumin induces down-regulation of c-FLIP and Mcl-1 expression

Next, we used human head and neck AMC-HN4 cells to identify the molecular mechanism of apoptosis. First, we investigated whether combined treatment with thioridazine and curcumin has a synergistic effect on apoptosis. Thioridazine plus curcumin has synergistically induced apoptosis in human head and neck AMC-HN4 cells (Fig. 3A). In addition, thioridazine plus curcumin induced chromatin damage in the nuclei (Fig. 3B) and DNA fragmentation (Fig. 3C). We also used Tamoxifen as reference drug (Fig. 3C). Furthermore, combined treatment with thioridazine and curcumin increased caspase activity (Fig. 3D), and apoptosis is markedly inhibited by a pan-caspase inhibitor (z-VAD) in thioridazine plus curcumin treated cells (Fig. 3E). To investigate the mechanism of apoptosis, we examined the modulation of apoptosis-related protein expression. Combined treatment with thioridazine and curcumin induced down-regulation of c-FLIP and Mcl-1 expression, but other apoptosis-related proteins (cIAP1, cIAP2, XIAP, Bcl-xL, and Bcl-2) did not change (Fig. 3F). Next, to identify the importance of c-FLIP and Mcl-1 down-regulation in apoptosis, cells were made to overexpress c-FLIP or Mcl-1. Ectopic expression of c-FLIP and Mcl-1 markedly inhibited apoptosis and cleavage of PARP (Fig. 4A and B). These results indicated that thioridazine plus curcumin induces caspase-mediated apoptosis through down-regulating c-FLIP and Mcl-1 protein expression.

3.3. Down-regulation of c-FLIP and Mcl-1 expression depends on augmentation of proteasome activity

Combined treatment with thioridazine and curcumin induced down-regulation of c-FLIP and Mcl-1 protein expression within 6h (Fig. 5A). However, the mRNA expression of c-FLIP and Mcl-1 did not change (Fig. 5B). Therefore, we investigated whether combined treatment with thioridazine and curcumin modulates protein stability using cycloheximide (CHX), an inhibitor of de novo protein synthesis. The expression levels of c-FLIP and Mcl-1 proteins are gradually down-regulated within 12 h in cells treated with CHX alone. However, both proteins are rapidly reduced within 3 h in the presence of thioridazine plus curcumin (Fig. 5C). Degradation of both c-FLIP and Mcl-1 expression is mainly mediated by the ubiquitin-proteasome pathway [44,45]. Therefore, we investigated the effect of proteasome inhibitors. Proteasome inhibitors (MG132 and lactacystine) reversed down-regulation of c-FLIP and Mcl-1 expression in thioridazine and curcumin-treated cells (Fig. 5D). In addition, combined treatment with thioridazine and curcumin increased proteasome activity (Fig. 5E). Therefore, our results suggested that thioridazine plus curcumin induced down-regulation of c-FLIP and Mcl-1 expression at the post-translational levels in a proteasome-dependent manner.

3.4. Up-regulation of PSMA5 expression plays a critical role in down-regulating c-FLIP and Mcl-1 expression

Up-regulation of proteasome subunit expression is related to augmentation of proteasome activity [46]. Therefore, we investigated whether thioridazine plus curcumin induced up-regulation of proteasome subunits. As shown in Fig. 6A and B, combined treatment with thioridazine and curcumin induced up-regulation of PSMA5 expression within 3 h; PSMA5 is a protein of the 20 S proteasome catalytic core. In contrast, thioridazine alone and curcumin alone had no effect (Fig. 6A). The mRNA expression of PSMA5 is up-regulated in cells treated with thioridazine plus curcumin (Fig. 6C). Furthermore, PSMA5 promoter activity is also induced by thioridazine plus curcumin treatment and sulforaphane (reference drug) treatment (Fig. 6D). Next, we
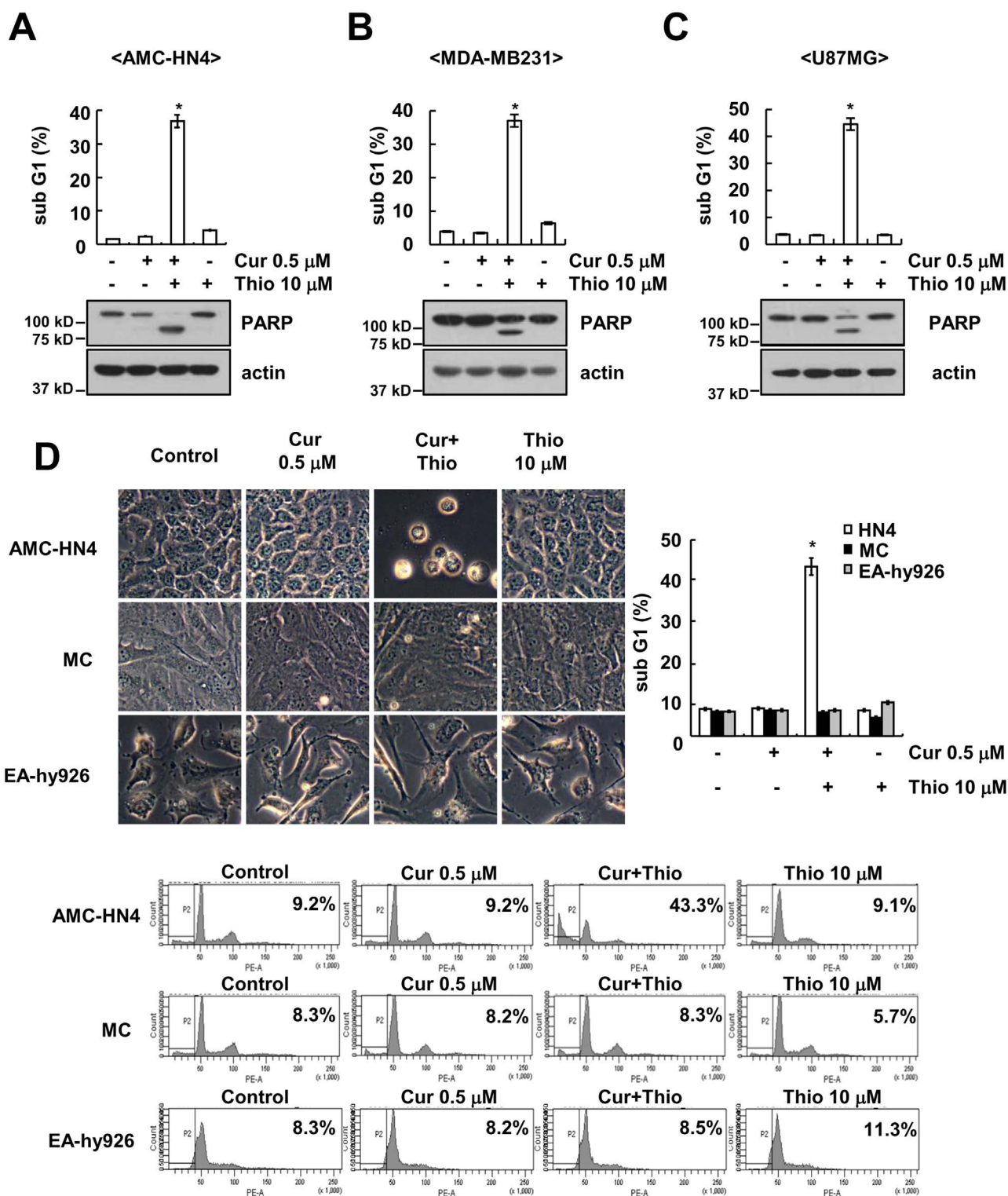
Fig. 2. Effect of combined treatment with thioridazine and curcumin on apoptosis in cancer cells and normal cells. (A–C) Human head and neck squamous cell carcinoma (AMC-HN4) (A), human breast carcinoma (MDA-MB231) (B), and human glioma (U87MG) (C) cells were treated with 10 µM thioridazine in the presence or absence of 0.5 µM curcumin for 24 h. The sub-G1 fraction was measured by flow cytometry. The protein expression levels of PARP and actin were determined by Western blot. The level of actin was used as a loading control. (D) AMC-HN4, human normal mesangial cells and normal human umbilical vein cells (EA.hy926) were treated with 10 µM thioridazine in the presence or absence of 0.5 µM curcumin for 24 h. The cell morphology was examined using interference light microscopy. The sub-G1 fraction and histogram were measured by flow cytometry. The values in A, B, C, and D represent the mean ± SD from three independent samples. * $p < 0.01$ compared to control.

investigated whether up-regulation of PSMA5 is involved in down-regulation of c-FLIP and Mcl-1 expression and apoptosis in thioridazine plus curcumin-treated cells. Down-regulation of PSMA5 by siRNA markedly inhibited thioridazine plus curcumin-induced apoptosis, cleavage of PARP, and down-regulation of c-FLIP and Mcl-1 expression (Fig. 6E). These results suggested that combined treatment with thioridazine and curcumin induced down-regulation of c-FLIP and Mcl-1 expression via up-regulating PSMA5 expression.
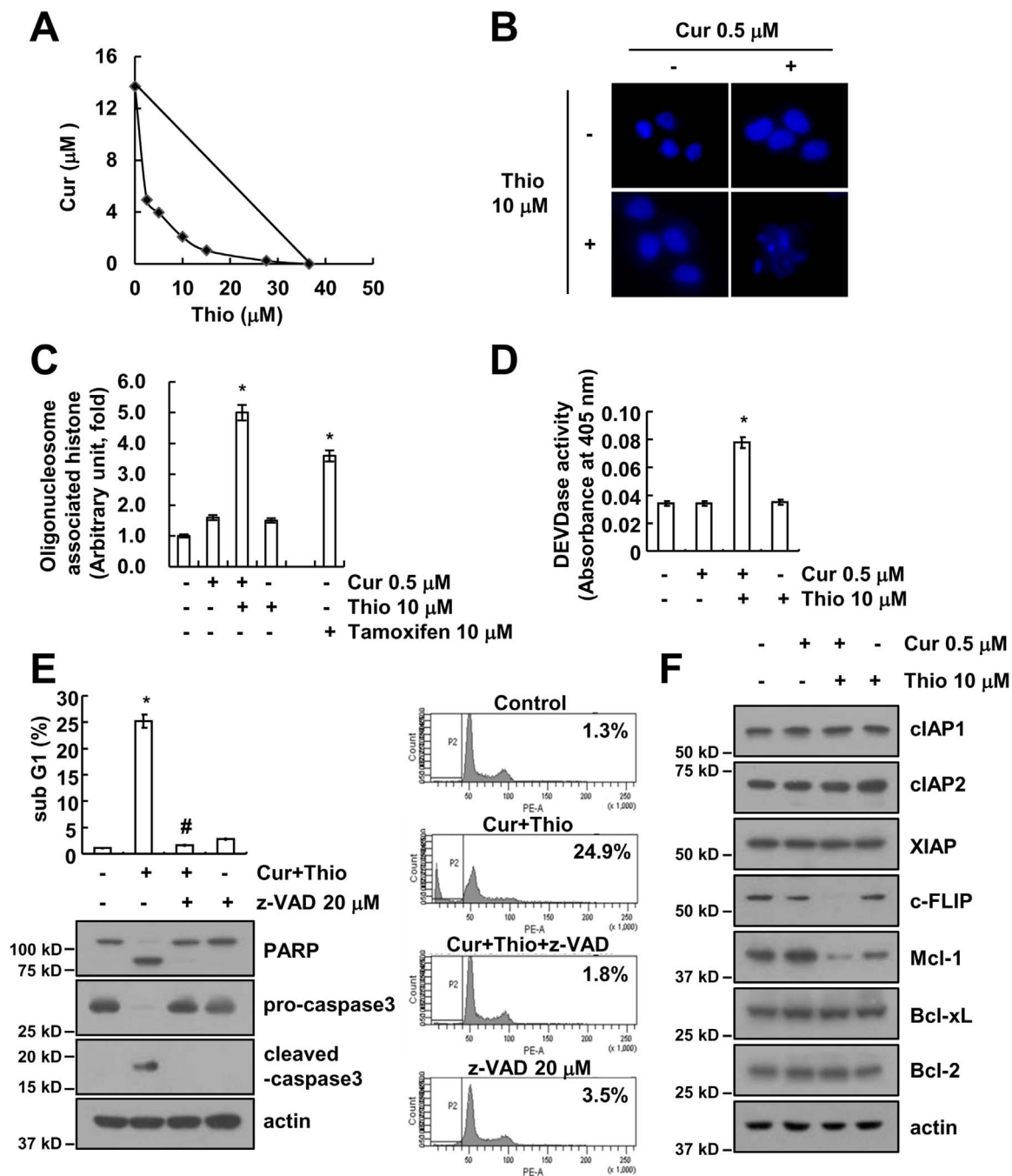
Fig. 3. Combined treatment with thioridazine and curcumin induces caspase-mediated apoptosis in human head and neck squamous cell carcinoma (AMC-HN4) cells. (A) Isoboles were obtained by plotting the combined concentrations of each drug required to produce 50% cell death. The straight line connecting the IC$_{50}$ values obtained for the two agents, when applied alone, corresponded to the addition of their independent effects. Values below this line indicate synergy, whereas values above this line indicate antagonism. (B–D) AMC-HN4 cells were treated with 10 μM thioridazine in the presence or absence of 0.5 μM curcumin for 24 h. The condensation and fragmentation of the nuclei were detected by 4′,6-diamidino-2-phenylindole staining (B). The cytoplasmic histone-associated DNA fragments were determined by a DNA fragmentation detection kit. Tamoxifen (10 μM, 24 h) was used as a positive control (C). Caspase activities were determined with colorimetric assays using caspase-3 (DEVDase) assay kits (D). (E) AMC-HN4 cells were treated with 10 μM thioridazine plus 0.5 μM curcumin for 24 h in the presence or absence of 20 μM z-VAD-fmk (z-VAD). The sub-G1 fraction and histogram were measured by flow cytometry. The protein expression levels of PARP, pro-caspase-3, cleaved caspase-3 and actin were determined by Western blot. The level of actin was used as a loading control. (F) AMC-HN4 cells were treated with 10 μM thioridazine in the presence or absence of 0.5 μM curcumin for 24 h. The protein expression levels of cIAP1, cIAP2, XIAP, c-FLIP, Mcl-1, Bcl-xL, Bcl-2 and actin were determined by Western blot. The level of actin was used as a loading control. The values in C, D and E represent the mean ± SD from three independent samples. * $p < 0.01$ compared to the control. # $p < 0.01$ compared to combined treatment with thioridazine and curcumin.

3.5. Up-regulation of PSMA5 expression depends on the Nrf2/ARE signaling pathway

Previous studies have reported that the promoter region of PSMA5 has an antioxidant response element (ARE), and nuclear translocation of Nrf2 induced up-regulation of PSMA5 expression [46]. Therefore, we

investigated whether Nrf2/ARE signaling is involved in PSMA5 expression in thioridazine plus curcumin-treated cells. Combined treatment with thioridazine and curcumin induced nuclear translocation of Nrf2 within 1 h as well as increased the ARE transcriptional activities (Fig. 7A and B). Combined treatment with thioridazine and curcumin showed similar levels of Nrf2 nuclear translocation and ARE
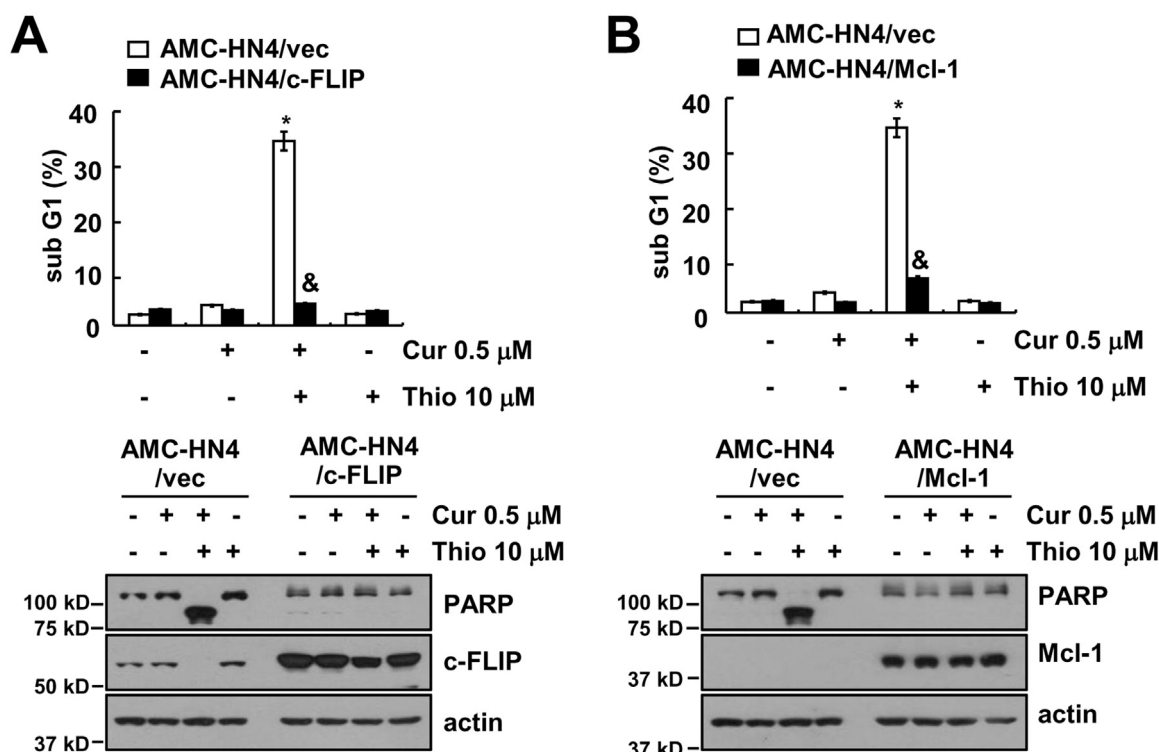
Fig. 4. Down-regulation of c-FLIP and Mcl-1 expression by thioridazine plus curcumin contributes to apoptosis. (A and B) AMC-HN4 cells were transiently transfected with pcDNA 3.1-c-FLIP (A) or pFLAG-CMV-4/Mcl-1 (B). Twenty-four hours after transfection, cells were treated with 10 μM thioridazine in the presence or absence of 0.5 μM curcumin for 24 h. The sub-G1 fraction was measured by flow cytometry. The protein expression levels of PARP, c-FLIP, Mcl-1 and actin were determined by Western blot. The level of actin was used as a loading control. The values in A and B represent the mean ± SD from three independent samples. * $p < 0.01$ compared to the control AMC-HN4/Vec. & $p < 0.01$ compared to thioridazine plus curcumin-treated AMC-HN4/Vec.

transcriptional activities compared with reference drug, sulforaphane (Fig. 7B and Supplementary material Fig. S1A). To confirm the involvement of Nrf2, we induced down-regulation of Nrf2 by siRNA. Down-regulation of Nrf2 inhibited apoptosis and PARP cleavage (Fig. 7C). Furthermore, up-regulation of PSMA5 expression and down-regulation of c-FLIP and Mcl-1 expression were reversed by down-regulation of Nrf2 (Fig. 7C). Our results suggested that Nrf2/ARE signaling is involved in thioridazine plus curcumin-induced apoptosis through up-regulation of PSMA5 expression.

3.6. Reactive oxygen species plays a critical role in thioridazine plus curcumin-induced apoptosis

Oxidative stress is one of the activators of the Nrf2/ARE signaling pathway. Therefore, we investigated whether thioridazine plus curcumin increased the intracellular reactive oxygen species (ROS) levels. Combined treatment with thioridazine and curcumin increased the ROS levels within 1 h (Fig. 8A). ROS scavengers [N-acetylcysteine (NAC), Glutathione-ethyl-ester (GEE), and trolox] inhibited nuclear translocation of Nrf2 in thioridazine plus curcumin-treated cells (Fig. 8B). ARE transcriptional activities and PSMA5 promoter activities are also blocked by ROS scavengers in thioridazine plus curcumin-treated cells (Fig. 8C and D). In addition, inhibition of ROS production prevented thioridazine plus curcumin-induced apoptosis, cleavage of PARP, and up-regulation of PSMA5 expression (Fig. 8E). Therefore, ROS are important in Nrf2/ARE-mediated PSMA5 expression in thioridazine plus curcumin-treated cells.

Next, we examined the source of ROS. First, we checked the effect of thioridazine plus curcumin on the mitochondrial ROS levels. However, thioridazine plus curcumin did not induce mitochondrial ROS levels (Fig. 9A). Furthermore, Mito-TEMPO, which is a specific mitochondrial superoxide scavenger, also had no effect on apoptosis; cleavage of PARP; or modulation of PSMA5, c-FLIP, and Mcl-1 expression (Fig. 9B).

Next, we checked the possibility of nicotinamide adenine dinucleotide phosphate (NADPH) oxidase (NOX) as an ROS source. The NOX inhibitors [diphenyleneiodonium (DPI) and apocynin] markedly inhibited apoptosis and cleavage of PARP, but not mitochondrial ROS inhibitor (rotenone), in thioridazine plus curcumin-treated cells (Fig. 9C). Furthermore, thioridazine plus curcumin-induced up-regulation of PSMA5 expression and down-regulation of c-FLIP and Mcl-1 were also reversed by NOX inhibitors (Fig. 9C). To further confirm the relation of NOX, we examined the NOX4 expression in thioridazine plus curcumin-treated cells. Curcumin plus thioridazine markedly induced NOX4 expression (Fig. 9D) and NBT reduction, which detects NOX4-dependent superoxide (Fig. 9E and Supplementary material Fig. S2A). Furthermore, we also confirmed ROS production by thioridazine plus curcumin using Amplex Red, cytoplasmic hydrogen peroxide sensor (Hyper-cyto), and GSSG/GSH measurement (Supplementary material Fig. S2B–D). Curcumin plus thioridazine induced hydrogen peroxide production and decreased GSH levels, but curcumin alone and thioridazine alone had no effect on NBT reduction, ROS production, and GSSG/GSH levels (Supplementary material Fig. S2A–D). In addition, down-regulation of NOX4 by siRNA blocked NBT reduction and inhibited apoptosis while modulating PSMA5, c-FLIP, and Mcl-1 expression (Fig. 9E and F). Therefore, these data suggested that thioridazine plus curcumin-induced ROS production is mediated by NOX4.

4. Discussion

Here, we demonstrated the mechanisms underlying combined treatment with thioridazine and curcumin-induced apoptosis in cancer cells. Thioridazine plus curcumin induced activation of Nrf2/ARE signaling pathways via NOX4-dependent ROS production. Activated Nrf2 increased PSMA5 expression at the transcriptional level and proteasome activity. Down-regulation of c-FLIP and Mcl-2 expression by augmentation of proteasome activity plays critical roles of thioridazine
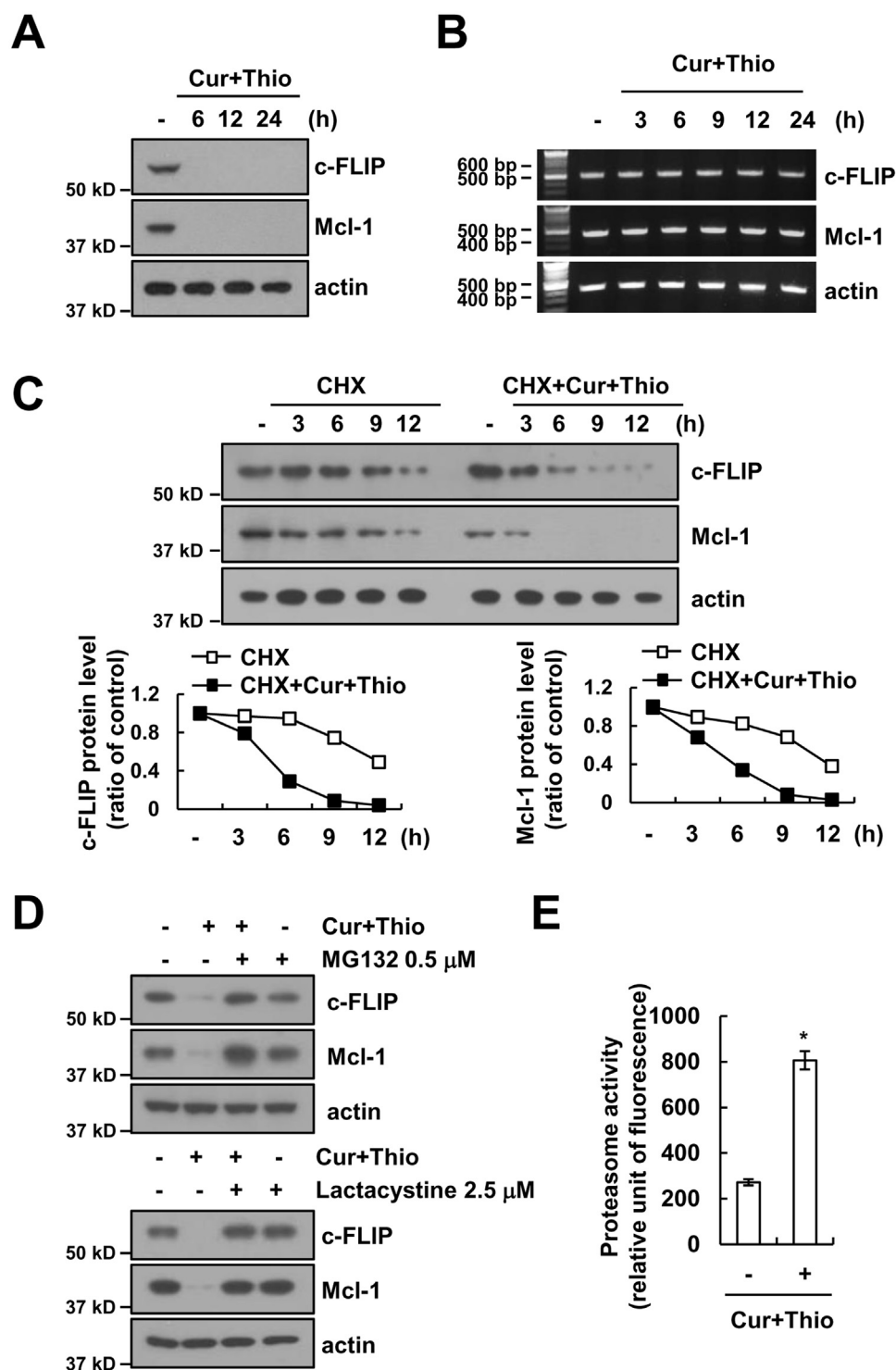
A

B

C

D

E

Fig. 5. Combined treatment with thioridazine and curcumin induces down-regulation of c-FLIP and Mcl-1 expression at the post-translational levels. (A and B) AMC-HN4 cells were treated with 10 μM thioridazine plus 0.5 μM curcumin for the indicated time periods. The protein (A) and mRNA (B) expression levels of c-FLIP, Mcl-1 and actin were determined by Western blot and RT-PCR, respectively. The level of actin was used as a loading control. (C) AMC-HN4 cells were treated with or without 10 μM thioridazine plus 0.5 μM curcumin in the presence of 20 μg/ml cyclohexamide (CHX) for the indicated time periods. The protein expression levels of c-FLIP, Mcl-1 and actin were determined by Western blot. The level of actin was used as a loading control. The band intensity of the c-FLIP and Mcl-1 protein was measured using ImageJ (public domain JAVA image-processing program ImageJ (http://rsb.info.nih.gov/ij)). (D) AMC-HN4 cells were pretreated with 0.5 μM MG132 and 2.5 μM lactacystin for 30 min; then, 10 μM thioridazine plus 0.5 μM curcumin was added for 24 h. The protein expression levels of c-FLIP, Mcl-1 and actin were determined by Western blot. The level of actin was used as a loading control. (E) AMC-HN4 cells were treated with 10 μM thioridazine plus 0.5 μM curcumin for 24 h. After treatment, the cells were lysed, and proteasome activity was measured as described in the Materials and Methods section. The values in E represent the mean ± SD from three independent samples. * $p < 0.01$ compared to control.

and curcumin-induced apoptosis. These results suggest that combined treatment with thioridazine and curcumin could be an effective anti-cancer strategy.

In our study, thioridazine plus curcumin induced apoptosis in a ROS-dependent manner (Fig. 8E). In our studies, while curcumin alone and thioridazine alone did not increase the intracellular ROS levels (Supplementary material Figs. S1C and S2), combined treatment with thioridazine and curcumin markedly increased the intracellular ROS levels (Fig. 8A and Supplementary material Fig. S2). However, an anti-cancer effect of curcumin in some cancer cells is mediated by up-regulation of ROS production. For example, curcumin (20 μM) produced

intracellular ROS and then induced ER stress-mediated apoptosis in cervical cancer [47], and curcumin (25 μM) induced apoptosis via ROS-mediated down-regulation of anti-apoptotic proteins (c-FLIP, Bcl-2, and c-IAP2) expression and inhibition of NF-κB signaling in T-cell lymphoma [48]. In contrast, curcumin also had an anti-oxidant function. The effect of curcumin on ROS production depends on the concentration [49]. Kang et al., reported that curcumin (< 20 μM) decreases the ROS levels, but curcumin (> 25 μM) increases the ROS levels in human hepatoma cells [49]. In our study, we used a very low dose of curcumin (0.5 μM), which might not induce ROS production or apoptosis. Thioridazine also acts as a pro-oxidant and anti-oxidant. Although
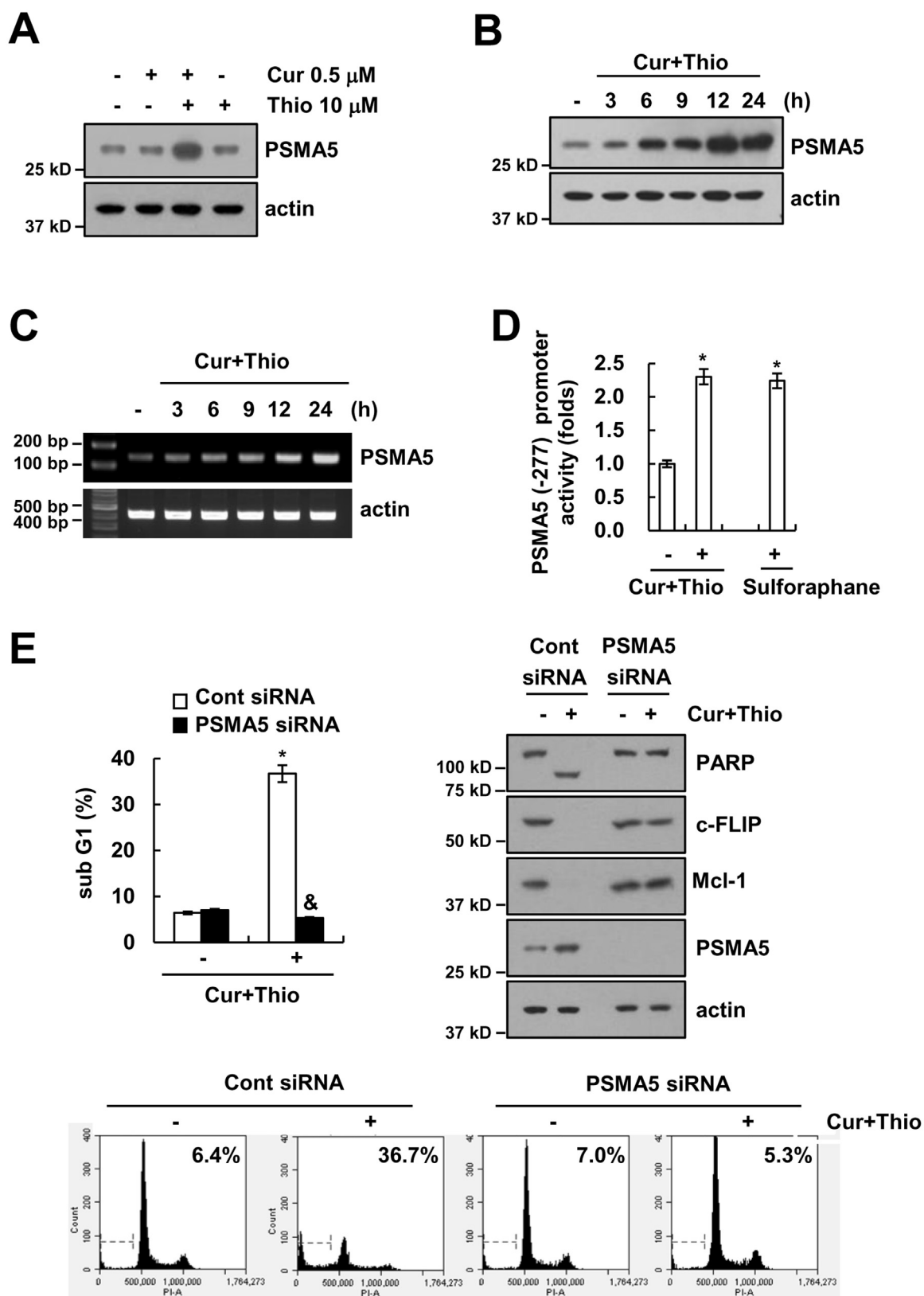
Fig. 6. Thioridazine plus curcumin induced up-regulation of PSMA5 expression. (A) AMC-HN4 cells were treated with 10 μM thioridazine in the presence or absence of 0.5 μM curcumin for 24 h. The protein expression levels of PSMA5 and actin were determined by Western blot. The level of actin was used as a loading control. (B and C) AMC-HN4 cells were treated with 10 μM thioridazine plus 0.5 μM curcumin for the indicated time periods. The protein (B) and mRNA (C) expression levels of PSMA5 and actin were determined by Western blot and RT-PCR, respectively. The level of actin was used as a loading control. (D) AMC-HN4 cells were transiently transfected with a plasmid harboring the luciferase gene under the control of the PSMA5/-277 promoter. After transfection, cells were treated with 10 μM thioridazine plus 0.5 μM curcumin for 24 h. The luciferase activity was analyzed. Sulforaphane (200 μM, 24 h) was used as a positive control. (E) AMC-HN4 cells were transiently transfected with a control siRNA or PSMA5 siRNA. Twenty-four hours after transfection, cells were treated with 10 μM thioridazine plus 0.5 μM curcumin for 24 h. The sub-G1 fraction and histogram were measured by flow cytometry as an indicator of the level of apoptosis. The protein expression levels of PARP, c-FLIP, Mcl-1, PSMA5 and actin were determined by Western blot. The level of actin was used as a loading control. The values in D and E represent the mean ± SD from three independent samples. * $p < 0.01$ compared to control. & $p < 0.01$ compared to thioridazine plus curcumin-treated control siRNA.
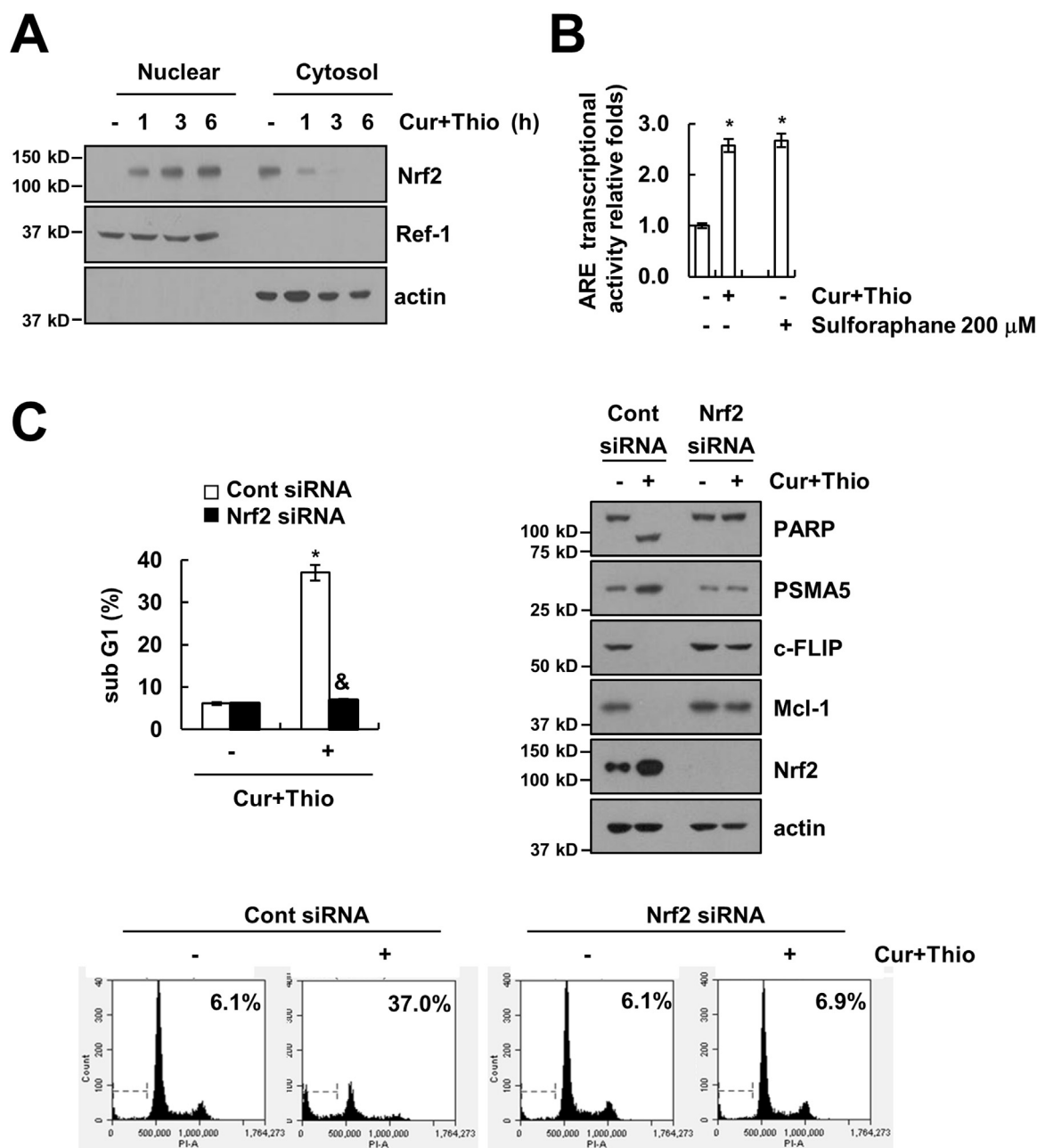
Fig. 7. Combined treatment with thioridazine and curcumin induced PSMA5 expression in an Nrf2-dependent manner. (A) AMC-HN4 cells were treated with 10 μM thioridazine plus 0.5 μM curcumin for the indicated time periods. After treatment, nuclear extracts and cytosolic extracts were analyzed for Nrf2 and Ref-1 by Western blot as described in the Section 2. (B) AMC-HN4 cells were transfected with an ARE-luciferase construct for 24 h, and cells were treated with 10 μM thioridazine plus 0.5 μM curcumin for 24 h. After treatment, cells were lysed and assayed for luciferase activity. Sulforaphane (200 μM, 24 h) was used as a positive control. (C) AMC-HN4 cells were transiently transfected with a control siRNA or Nrf2 siRNA. Twenty-four hours after transfection, cells were treated with 10 μM thioridazine plus 0.5 μM curcumin for 24 h. The sub G1 fraction and histogram were measured by flow cytometry as an indicator of the level of apoptosis. The protein expression levels of PARP, PSMA5, c-FLIP, Mcl-1, Nrf2 and actin were determined by Western blot. The values in B and C represent the mean ± SD from three independent samples. * $p < 0.01$ compared to control. & $p < 0.01$ compared to thioridazine plus curcumin-treated control siRNA.

thioridazine (10 μM) did not increase the ROS levels in human head and neck carcinoma cells (Supplementary material Figs. S1C and S2), the same dosage of thioridazine markedly increased ROS production in human renal carcinoma Caki cells [16]. In contrast, thioridazine (10 μM) inhibited the accumulation of superoxide produced by the respiratory chain in mitochondria [50]. Therefore, ROS production by thioridazine depends on the cell types and contexts.

Many anti-cancer drugs induce cell death through up-regulating the intracellular ROS levels. One of intracellular ROS sources is nicotinamide adenosine dinucleotide phosphate (NADPH) oxidase (NOX). In our study, we suggested that NOX4 plays a major role in combined treatment with curcumin and thioridazine-induced ROS production.

First, combined treatment with curcumin and thioridazine induced up-regulation of NOX4 expression (Fig. 9D), and knock-down of NOX4 by siRNA markedly inhibited apoptosis (Fig. 9F). NOX4 activity is mainly determined by NOX4 protein expression [51]. Second, we found that down-regulation of NOX4 by siRNA markedly inhibited ROS production and Nrf2 nuclear translocation in curcumin plus thioridazine treated cells (Fig. 9E, Supplementary material Figs. S1D and S2B–D). In addition, we investigated the effect of NOXs on curcumin plus thioridazine-induced ROS production and modulation of c-FLIP, Mcl-1, and PSMA5 expression. The NOX inhibitors (DPI, apocynin, and VAS2870) and NOX1/4 inhibitor (GKT137831) inhibited ROS production and down-regulation of c-FLIP and Mcl-1 expression and up-regulation of PSMA5
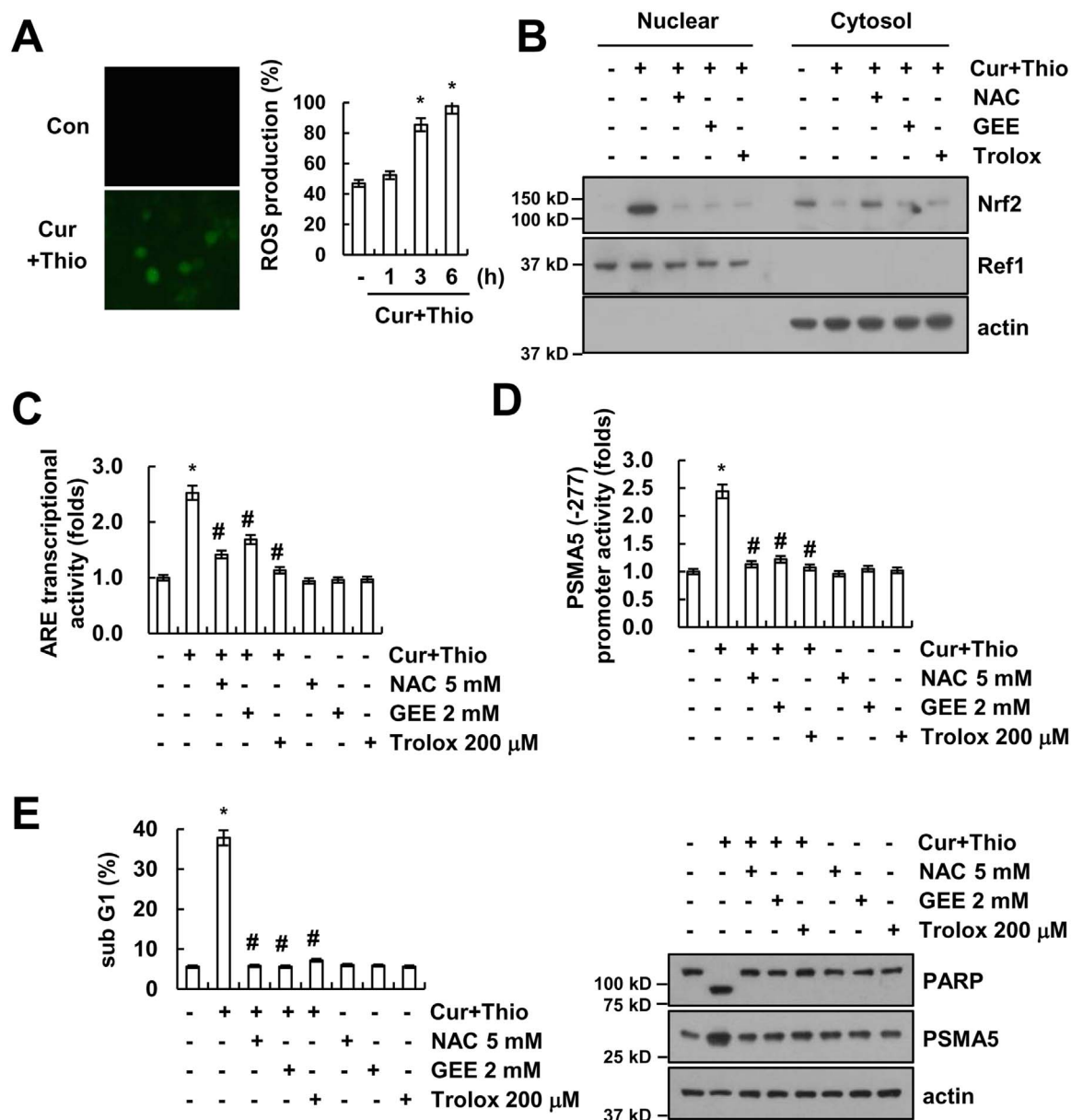
Fig. 8. Reactive oxygen species play a critical role in thioridazine plus curcumin-mediated PSMA5 expression. (A) AMC-HN4 cells were treated with 10 µM thioridazine plus 0.5 µM curcumin for 6 h (left panel) for the indicated time periods (right panel), and the cells were then loaded with H_2DCF-DA fluorescent dye. The H_2DCF-DA fluorescence intensity was detected by a fluorescence microscope (left panel) and flow cytometry (right panel). (B) AMC-HN4 cells were pretreated with 5 mM NAC, 2 mM GEE, and 200 µM trolox for 30 min, and they were then treated with 10 µM thioridazine plus 0.5 µM curcumin for 24 h. After treatment, nuclear extracts were analyzed for Nrf2 and Ref-1 by Western blot as described in the Section 2. Ref1 was used as a marker of the nuclear fraction. (C–D) AMC-HN4 cells were transfected with an ARE-luciferase construct (C) or a plasmid harboring the luciferase gene under the control of the PSMA5/-277 promoter (D). After transfection, cells were pretreated with 5 mM NAC, 2 mM GEE, and 200 µM trolox for 30 min, and they were then treated with 10 µM thioridazine plus 0.5 µM curcumin for 24 h. After treatment, cells were lysed and assayed for luciferase activity. (E) AMC-HN4 cells were pretreated with 5 mM NAC, 2 mM GEE, and 200 µM trolox for 30 min, and they were then treated with 10 µM thioridazine plus 0.5 µM curcumin for 24 h. The sub-G1 fraction was measured by flow cytometry. The protein expression levels of PARP, PSMA5 and actin were determined by Western blot. The level of actin was used as a loading control. The values in A, C, D and E represent the mean ± SD from three independent samples. * $p < 0.01$ compared to control. # $p < 0.01$ compared to thioridazine plus curcumin.

expression in curcumin plus thioridazine-treated cells (Supplementary material Fig. S3). However, NOX1 inhibitor (ML171) and NOX2 inhibitor (Phox-I2) had no effect (Supplementary material Fig. S3). Therefore, NOX4 plays a critical role in curcumin plus thioridazine-induced ROS production.

Thioridazine is one of phenothiazines families, which has an anti-psychotic drug depending on inhibition of dopaminergic D2 receptors. The bioavailability of thioridazine showed great variability, ranged from 25% to 33%, and oral administration of thioridazine (100 mg) reached maximal concentration (371.8 ng/ml) in the plasma between 1 and 2 h [52]. High concentrations of thioridazine, as anti-psychotic drug have side effects such as dysrhythmia, sudden death, anti-hERG

activity and strong sedative effects [53–55]. Therefore, to reduce side effects we used combined treatment with low concentrations of thioridazine and curcumin. Thioridazine inhibits cellular ROS production via inhibition of NOX enzymes. Based on structures, N-substituted phenothiazines, such as thioridazine, inhibited NOX enzymes, but unsubstituted phenothiazines had no effect on NOX activity [56]. Thioridazine inhibits NOX2 with an IC_{50} of 0.5–2 µM [57]. Lena et al. reported that thioridazine inhibited NOX4 with an IC_{50} of 5 µM in tetracycline-induced T-Rex™ NOX4 cells [51]. In our study, as shown in Supplementary material Fig. S1C, thioridazine alone or curcumin alone did not effect on NOX4 expression. However, combined treatment with thioridazine and curcumin significantly induced NOX4 expression
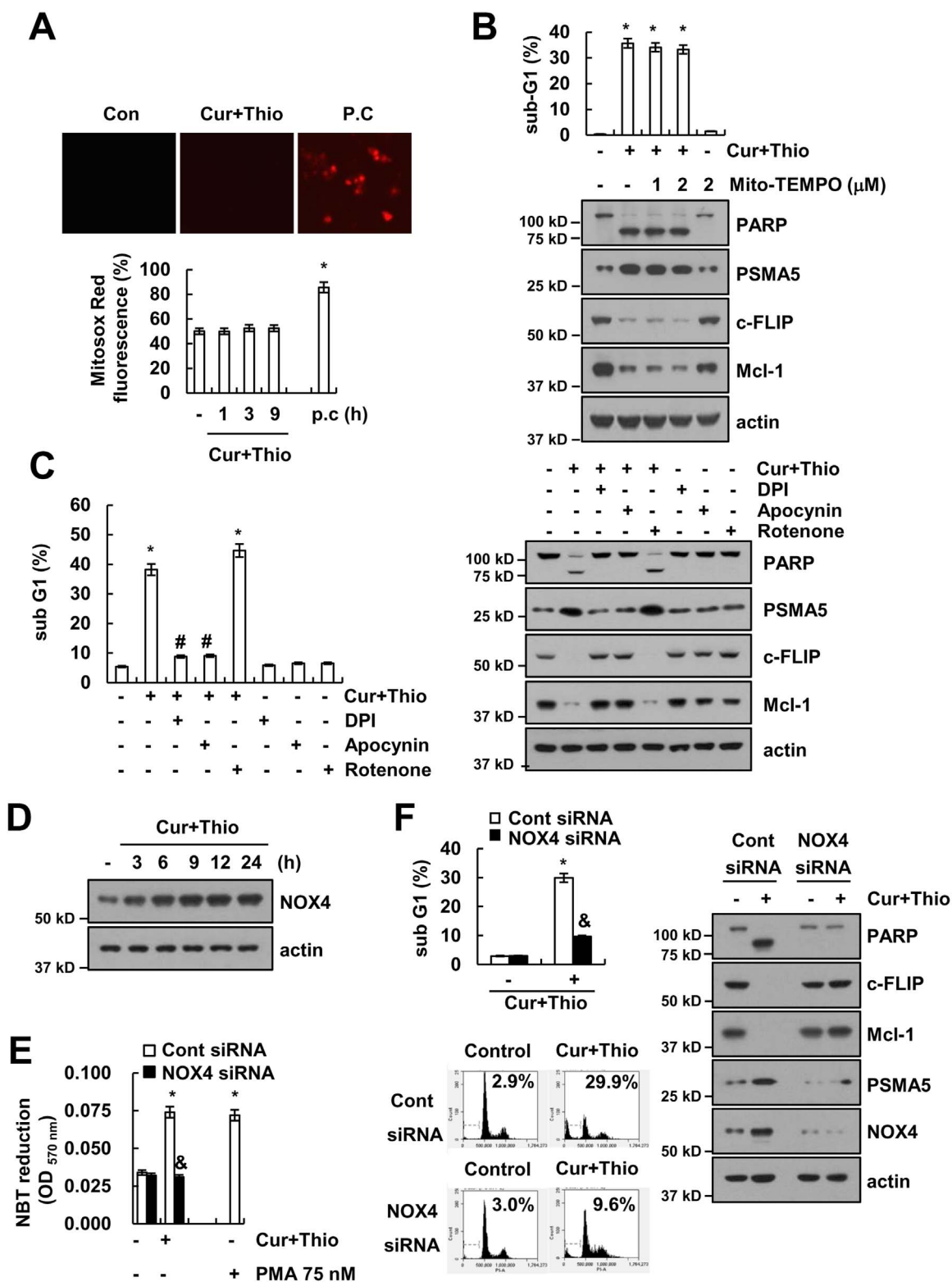
(caption on next page)

In addition, NOX4 siRNA markedly reduced curcumin plus thioridazine-induced ROS production. Therefore, these results suggest that thioridazine's inhibitory effect of NOX4 activity did not much effect on curcumin plus thioridazine-induced ROS production in our systems. We need further experiments to identify the effect of thioridazine on NOX4 enzyme activity in AMC-HN4 cells.

Several papers reported that curcumin has been known as a safe compound at high dose [58,59]. When mice were treated with curcumin by gavage (0.4 μmol), intraperitoneal (i.p.) (0.4 μmol) or intramuscular (i.m.) (0.2 μmol), curcumin was detected 0.519 μg/g, 0.739 μg/g, or 1.162 μg/g in the brain, respectively [60] and curcumin easily crosses the blood brain barrier [61,62]. In addition, when orally administered with 400 mg curcumin in the rats, only about 60% of curcumin was absorbed, and very low levels of the curcumin in liver

Fig. 9. Up-regulation of NOX4 expression is associated with increased ROS levels in thioridazine plus curcumin-treated cells. (A) AMC-HN4 cells were treated with 10 μM thioridazine plus 0.5 μM curcumin or 2 μM cathepsin S inhibitor (Z-FL-COCHO; positive control) for 3 h (upper panel) for the indicated time periods (lower panel). Cells were then loaded with Mitosox Red fluorescent dye. The Mitosox Red fluorescence intensity was detected by a fluorescence microscope (upper panel) and flow cytometry (lower panel). (B) AMC-HN4 cells were pretreated with the indicated concentrations of Mito-TEMPO, and they were then treated with 10 μM thioridazine plus 0.5 μM curcumin for 24 h. The sub-G1 fraction was measured by flow cytometry. The protein expression levels of PARP, PSMA5, c-FLIP, Mcl-1 and actin were determined by Western blot. The level of actin was used as a loading control. (C) AMC-HN4 cells were pretreated with 100 μM apocynin, 100 nM DPI and 20 nM rotenone for 30 min, which was followed by stimulation with 10 μM thioridazine plus 0.5 μM curcumin for 24 h. The sub-G1 fraction was measured by flow cytometry. The protein expression levels of PARP, PSMA5, c-FLIP, Mcl-1 and actin were determined by Western blot. The level of actin was used as a loading control. (D) AMC-HN4 cells were treated with 10 μM thioridazine plus 0.5 μM curcumin for the indicated time periods. The protein expression levels of NOX4 and actin were determined by Western blot. The level of actin was used as a loading control. (E) AMC-HN4 cells were transiently transfected with a control siRNA or NOX4 siRNA. Twenty-four hours after transfection, cells were treated with 10 μM thioridazine plus 0.5 μM curcumin for 12 h. PMA (75 nM, 12 h) was used as a positive control. The NBT reduction was detected by absorbance quantification at 570 nm. (F) AMC-HN4 cells were transiently transfected with a control siRNA or NOX4 siRNA. Twenty-four hours after transfection, cells were treated with 10 μM thioridazine plus 0.5 μM curcumin for 24 h. The sub G1 fraction was measured by flow cytometry as an indicator of the level of apoptosis. The protein expression levels of PARP, c-FLIP, Mcl-1, PSMA5, NOX4 and actin were determined by Western blot. The values in A, B, C, E and F represent the mean ± SD from three independent samples. * $p < 0.01$ compared to control. # $p < 0.01$ compared to thioridazine plus curcumin. & $p < 0.01$ compared to thioridazine plus curcumin-treated control siRNA.

---

and kidney (< 20 μg/tissue) were detected from 15 min up to 24 h [63]. Furthermore, when the curcumin (0.1 g/kg) was administrated by i.p. in the mice, the levels of curcumin in the intestines, spleen, liver, and kidneys after 1 h was detected 177.04, 26.06, 26.90, and 7.51 μg/g, respectively [64]. Recently, to increase the bioavailability of curcumin, curcumin hydrogel was used. After intranasal administration of the curcumin hydrogel, the levels of curcumin in the cerebrum, cerebellum, hippocampus and olfactory bulb were higher than i.v. administration [65]. Clinical trials of oral curcumin have a limitation, because most of curcumin underdoes metabolism in intestine and liver. To improve the bioavailability of curcumin, piperine which is an inhibitor of hepatic and intestinal glucuronidation, increase 2000% increase bioavailability of curcumin [66], and micronized powder and liquid micelles markedly induced better bioavailability than native curcumin [67]. There are reported about anti-cancer effects of curcumin in multiple cancers, however, the information about the bioavailability of curcumin in head and neck cancer is unknown. Furthermore, curcumin has been classified as a PAINS (pan-assay interference compounds) and an IMP (invalid metabolic panaceas) [68]. Therefore, combined treatment with curcumin and other anti-cancer drugs could reduce toxicity and enhance anti-cancer effects.

In our studies, combined treatment with thioridazine and curcumin induced down-regulation of c-FLIP through up-regulation of ROS-mediated PSMA5 expression (Fig. 6E). In addition, ROS plays critical roles on down-regulation of c-FLIP expression via multiple mechanisms. First, ROS induces expression levels of Cbl, E3 ligase of c-FLIP. Seo et al., reported that inhibition of cathepsin S induced down-regulation of c-FLIP expression through up-regulation of Cbl expression in a ROS-dependent manner [69]. Second, ROS induces phosphorylation and ubiquitination of c-FLIP. ROS inducers (menadione, paraquat, and buthionine sulfoximine) increased phosphorylation at Thr 166, and then enhanced ubiquitination at Lys 167 of c-FLIP [70]. In contrast, nitric oxide induced *S*-nitrosylation of c-FLIP inhibits ubiquitination. Chanvorachote et al., reported that Cys 254 and Cys 259 are the principle target sites for *S*-nitrosylation of c-FLIP [71]. In case of Mcl-1, phosphorylation status determines the stability of Mcl-1. The ERK-mediated phosphorylation of Thr 92 and Thr 163 residue and JNK-mediated phosphorylation of Ser 121 and Thr 163 residue enhance stabilization of Mcl-1 [72–74]. Interestingly, phosphorylation at Thr 163, Ser159 and Ser155 by glycogen synthase kinase (GSK)-3 is required for degradation of Mcl-1 [75]. However, role of ROS in Mcl-1 protein stability is not well known. In previous study, thioridazine induced ROS-mediated down-regulation of Mcl-1 expression in human renal carcinoma Caki cells [16]. However, thioridazine did not induce PSMA5 expression [16]. Therefore, modulation of c-FLIP and Mcl-1 protein expression is mediated via multiple mechanisms in a cell text and stimuli-dependent manner.

Taken together, we suggest that combined treatment with curcumin and thioridazine induced apoptosis through down-regulating c-FLIP and Mcl-1 expression at the post-translational levels by NOX4-mediated up-regulation of proteasome activity. Therefore, combined treatment with thioridazine and curcumin could facilitate the development of a

safe and an effective strategy for cancer treatment.

Conflicts of interest

The authors declare no conflicts of interest.

Appendix A. Supplementary material

Supplementary data associated with this article can be found in the online version at http://dx.doi.org/10.1016/j.redox.2017.07.017.

References

[1] G.M. Realmuto, W.D. Erickson, A.M. Yellin, J.H. Hopwood, L.M. Greenberg, Clinical comparison of thiothixene and thioridazine in schizophrenic adolescents, Am. J. Psychiatry 141 (1984) 440–442.

[2] R. Ohman, R. Axelsson, Relationship between prolactin response and antipsychotic effect of thioridazine in psychiatric patients, Eur. J. Clin. Pharmacol. 14 (1978) 111–116.

[3] S. Kang, S.M. Dong, B.R. Kim, M.S. Park, B. Trink, H.J. Byun, S.B. Rho, Thioridazine induces apoptosis by targeting the PI3K/Akt/mTOR pathway in cervical and endometrial cancer cells, Apoptosis 17 (2012) 989–997.

[4] S.B. Rho, B.R. Kim, S. Kang, A gene signature-based approach identifies thioridazine as an inhibitor of phosphatidylinositol-3′-kinase (PI3K)/AKT pathway in ovarian cancer cells, Gynecol. Oncol. 120 (2011) 121–127.

[5] D. Nagel, S. Spranger, M. Vincendeau, M. Grau, S. Raffegerst, B. Kloo, D. Hlahla, M. Neuenschwander, J. Peter von Kries, K. Hadian, B. Dorken, P. Lenz, G. Lenz, D.J. Schendel, D. Krappmann, Pharmacologic inhibition of MALT1 protease by phenothiazines as a therapeutic approach for the treatment of aggressive ABC-DLBCL, Cancer Cell 22 (2012) 825–837.

[6] I. Gil-Ad, B. Shtaif, Y. Levkovitz, M. Dayag, E. Zeldich, A. Weizman, Characterization of phenothiazine-induced apoptosis in neuroblastoma and glioma cell lines: clinical relevance and possible application for brain-derived tumors, J. Mol. Neurosci. 22 (2004) 189–198.

[7] Z. Zhelev, H. Ohba, R. Bakalova, V. Hadjimitova, M. Ishikawa, Y. Shinohara, Y. Baba, Phenothiazines suppress proliferation and induce apoptosis in cultured leukemic cells without any influence on the viability of normal lymphocytes, Phenothiazines Leuk. Cancer Chemother. Pharmacol. 53 (2004) 267–275.

[8] I. Gil-Ad, B. Shtaif, Y. Levkovitz, J. Nordenberg, M. Taler, I. Korov, A. Weizman, Phenothiazines induce apoptosis in a B16 mouse melanoma cell line and attenuate in vivo melanoma tumor growth, Oncol. Rep. 15 (2006) 107–112.

[9] M.S. Park, S.M. Dong, B.R. Kim, S.H. Seo, S. Kang, E.J. Lee, S.H. Lee, S.B. Rho, Thioridazine inhibits angiogenesis and tumor growth by targeting the VEGFR-2/PI3K/mTOR pathway in ovarian cancer xenografts, Oncotarget 5 (2014) 4929–4934.

[10] H.J. Byun, J.H. Lee, B.R. Kim, S. Kang, S.M. Dong, M.S. Park, S.H. Lee, S.H. Park, S.B. Rho, Anti-angiogenic effects of thioridazine involving the FAK-mTOR pathway, Microvasc. Res. 84 (2012) 227–234.

[11] M. Lu, J. Li, Z. Luo, S. Zhang, S. Xue, K. Wang, Y. Shi, C. Zhang, H. Chen, Z. Li, Roles of dopamine receptors and their antagonist thioridazine in hepatoma metastasis, Onco Targets Ther. 8 (2015) 1543–1552.

[12] E. Sachlos, R.M. Risueno, S. Laronde, Z. Shapovalova, J.H. Lee, J. Russell, M. Malig, J.D. McNicol, A. Fiebig-Comyn, M. Graham, M. Levadoux-Martin, J.B. Lee, A.O. Giacomelli, J.A. Hassell, D. Fischer-Russell, M.R. Trus, R. Foley, B. Leber, A. Xenocostas, E.D. Brown, T.J. Collins, M. Bhatia, Identification of drugs including a dopamine receptor antagonist that selectively target cancer stem cells, Cell 149

(2012) 1284–1297.

[13] H. Yue, D. Huang, L. Qin, Z. Zheng, L. Hua, G. Wang, J. Huang, H. Huang, Targeting lung cancer stem cells with antipsychological drug thioridazine, Biomed. Res. Int. 2016 (2016) 6709828–6709844.

[14] S. Ronald, S. Awate, A. Rath, J. Carroll, F. Galiano, D. Dwyer, H. Kleiner-Hancock, J.M. Mathis, S. Vigod, A. De Benedetti, Phenothiazine Inhibitors of TLKs affect double-strand break repair and DNA damage response recovery and potentiate tumor killing with radiomimetic therapy, Genes Cancer 4 (2013) 39–53.

[15] J.S. Strobl, K.L. Kirkwood, T.K. Lantz, M.A. Lewine, V.A. Peterson, J.F. Worley 3rd, Inhibition of human breast cancer cell proliferation in tissue culture by the neuroleptic agents pimozide and thioridazine, Cancer Res. 50 (1990) 5399–5405.

[16] K.J. Min, B.R. Seo, Y.C. Bae, Y.H. Yoo, T.K. Kwon, Antipsychotic agent thioridazine sensitizes renal carcinoma Caki cells to TRAIL-induced apoptosis through reactive oxygen species-mediated inhibition of Akt signaling and downregulation of Mcl-1 and c-FLIP(L), Cell Death Dis. 5 (2014) e1063–e1071.

[17] X.Y. Ke, V.W. Lin, Ng, S.J. Gao, Y.W. Tong, J.L. Hedrick, Y.Y. Yang, Co-delivery of thioridazine and doxorubicin using polymeric micelles for targeting both cancer cells and cancer stem cells, Biomaterials 35 (2014) 1096–1108.

[18] X. Jin, B. Zou, L. Luo, C. Zhong, P. Zhang, H. Cheng, Y. Guo, M. Gou, Codelivery of thioridazine and doxorubicin using nanoparticles for effective breast cancer therapy, Int. J. Nanomed. 11 (2016) 4545–4552.

[19] S.S. Han, S.T. Chung, D.A. Robertson, D. Ranjan, S. Bondada, Curcumin causes the growth arrest and apoptosis of B cell lymphoma by downregulation of egr-1, c-myc, bcl-XL, NF-kappa B, and p53, Clin. Immunol. 93 (1999) 152–161.

[20] H. Chen, Z.S. Zhang, Y.L. Zhang, D.Y. Zhou, Curcumin inhibits cell proliferation by interfering with the cell cycle and inducing apoptosis in colon carcinoma cells, Anticancer Res. 19 (1999) 3675–3680.

[21] L. Moragoda, R. Jaszewski, A.P. Majumdar, Curcumin induced modulation of cell cycle and apoptosis in gastric and colon cancer cells, Anticancer Res. 21 (2001) 873–878.

[22] S. Pal, T. Choudhuri, S. Chattopadhyay, A. Bhattacharya, G.K. Datta, T. Das, G. Sa, Mechanisms of curcumin-induced apoptosis of Ehrlich's ascites carcinoma cells, Biochem. Biophys. Res. Commun. 288 (2001) 658–665.

[23] J.A. Bush, K.J. Cheung Jr., G. Li, Curcumin induces apoptosis in human melanoma cells through a Fas receptor/caspase-8 pathway independent of p53, Exp. Cell Res. 271 (2001) 305–314.

[24] A.C. Bharti, N. Donato, S. Singh, B.B. Aggarwal, Curcumin (diferuloylmethane) down-regulates the constitutive activation of nuclear factor-kappa B and IkappaBalpha kinase in human multiple myeloma cells, leading to suppression of proliferation and induction of apoptosis, Blood 101 (2003) 1053–1062.

[25] Z. Fu, X. Chen, S. Guan, Y. Yan, H. Lin, Z.C. Hua, Curcumin inhibits angiogenesis and improves defective hematopoiesis induced by tumor-derived VEGF in tumor model through modulating VEGF-VEGFR2 signaling pathway, Oncotarget 6 (2015) 19469–19482.

[26] G. Chakraborty, S. Jain, S. Kale, R. Raja, S. Kumar, R. Mishra, G.C. Kundu, Curcumin suppresses breast tumor angiogenesis by abrogating osteopontin-induced VEGF expression, Mol. Med. Rep. 1 (2008) 641–646.

[27] L. Cao, J. Liu, L. Zhang, X. Xiao, W. Li, Curcumin inhibits H2O2-induced invasion and migration of human pancreatic cancer via suppression of the ERK/NF-kappaB pathway, Oncol. Rep. 36 (2016) 2245–2251.

[28] M. He, D. Wang, D. Zou, C. Wang, B. Lopes-Bastos, W.G. Jiang, J. Chester, Q. Zhou, J. Cai, Re-purposing of curcumin as an anti-metastatic agent for the treatment of epithelial ovarian cancer: in vitro model using cancer stem cell enriched ovarian cancer spheroids, Oncotarget 7 (2016) 86374–86387.

[29] D. Deeb, Y.X. Xu, H. Jiang, X. Gao, N. Janakiraman, R.A. Chapman, S.C. Gautam, Curcumin (diferuloyl-methane) enhances tumor necrosis factor-related apoptosis-inducing ligand-induced apoptosis in LNCaP prostate cancer cells, Mol. Cancer Ther. 2 (2003) 95–103.

[30] E.M. Jung, J.H. Lim, T.J. Lee, J.W. Park, K.S. Choi, T.K. Kwon, Curcumin sensitizes tumor necrosis factor-related apoptosis-inducing ligand (TRAIL)-induced apoptosis through reactive oxygen species-mediated upregulation of death receptor 5 (DR5), Carcinogenesis 26 (2005) 1905–1913.

[31] X. Gao, D. Deeb, H. Jiang, Y.B. Liu, S.A. Dulchavsky, S.C. Gautam, Curcumin differentially sensitizes malignant glioma cells to TRAIL/Apo2L-mediated apoptosis through activation of procaspases and release of cytochrome c from mitochondria, J. Exp. Ther. Oncol. 5 (2005) 39–48.

[32] B.S. Vinod, J. Antony, H.H. Nair, V.T. Puliyappadamba, M. Saikia, S.S. Narayanan, A. Bevin, R.J. Anto, Mechanistic evaluation of the signaling events regulating curcumin-mediated chemosensitization of breast cancer cells to 5-fluorouracil, Cell Death Dis. 4 (2013) e505–e517.

[33] A.B. Kunnumakkara, S. Guha, S. Krishnan, P. Diagaradjane, J. Gelovani, B.B. Aggarwal, Curcumin potentiates antitumor activity of gemcitabine in an orthotopic model of pancreatic cancer through suppression of proliferation, angiogenesis, and inhibition of nuclear factor-kappaB-regulated gene products, Cancer Res. 67 (2007) 3853–3861.

[34] S.K. Sandur, A. Deorukhkar, M.K. Pandey, A.M. Pabon, S. Shentu, S. Guha, B.B. Aggarwal, S. Krishnan, Curcumin modulates the radiosensitivity of colorectal cancer cells by suppressing constitutive and inducible NF-kappaB activity, Int. J. Radiat. Oncol. Biol. Phys. 75 (2009) 534–542.

[35] A.B. Kunnumakkara, P. Diagaradjane, S. Guha, A. Deorukhkar, S. Shentu, B.B. Aggarwal, S. Krishnan, Curcumin sensitizes human colorectal cancer xenografts in nude mice to gamma-radiation by targeting nuclear factor-kappaB-regulated gene products, Clin. Cancer Res. 14 (2008) 2128–2136.

[36] H.J. Um, T.K. Kwon, Protective effect of melatonin on oxaliplatin-induced apoptosis through sustained Mcl-1 expression and anti-oxidant action in renal carcinoma Caki cells, J. Pineal Res. 49 (2010) 283–290.

[37] S. Kim, T.J. Lee, J. Leem, K.S. Choi, J.W. Park, T.K. Kwon, Sanguinarine-induced apoptosis: generation of ROS, down-regulation of Bcl-2, c-FLIP, and synergy with TRAIL, J. Cell. Biochem. 104 (2008) 895–907.

[38] R.J. Tallarida, Drug synergism: its detection and applications, J. Pharmacol. Exp. Ther. 298 (2001) 865–872.

[39] Y.A. An, J.Y. Hwang, J.S. Lee, Y.C. Kim, Cornus officinalis methanol extract upregulates melanogenesis in melan-a cells, Toxicol. Res. 31 (2015) 165–172.

[40] M.G. Dilshara, C.H. Kang, Y.H. Choi, G.Y. Kim, Mangiferin inhibits tumor necrosis factor-alpha-induced matrix metalloproteinase-9 expression and cellular invasion by suppressing nuclear factor-kappaB activity, BMB Rep. 48 (2015) 559–564.

[41] F. Tietze, Enzymic method for quantitative determination of nanogram amounts of total and oxidized glutathione: applications to mammalian blood and other tissues, Anal. Biochem. 27 (1969) 502–522.

[42] T.P. Akerboom, H. Sies, Assay of glutathione, glutathione disulfide, and glutathione mixed disulfides in biological samples, Methods Enzymol. 77 (1981) 373–382.

[43] M.E. Anderson, Determination of glutathione and glutathione disulfide in biological samples, Methods Enzymol. 113 (1985) 548–555.

[44] Q. Zhong, W. Gao, F. Du, X. Wang, Mule/ARF-BP1, a BH3-only E3 ubiquitin ligase, catalyzes the polyubiquitination of Mcl-1 and regulates apoptosis, Cell 121 (2005) 1085–1095.

[45] T. Fukazawa, T. Fujiwara, F. Uno, F. Teraishi, Y. Kadowaki, T. Itoshima, Y. Takata, S. Kagawa, J.A. Roth, J. Tschopp, N. Tanaka, Accelerated degradation of cellular FLIP protein through the ubiquitin-proteasome pathway in p53-mediated apoptosis of human cancer cells, Oncogene 20 (2001) 5225–5231.

[46] A. Arlt, I. Bauer, C. Schafmayer, J. Tepel, S.S. Muerkoster, M. Brosch, C. Roder, H. Kalthoff, J. Hampe, M.P. Moyer, U.R. Folsch, H. Schafer, Increased proteasome subunit protein expression and proteasome activity in colon cancer relate to an enhanced activation of nuclear factor E2-related factor 2 (Nrf2), Oncogene 28 (2009) 3983–3996.

[47] B. Kim, H.S. Kim, E.J. Jung, J.Y. Lee, B. K.T, J.M. Lim, Y.S. Song, Curcumin induces ER stress-mediated apoptosis through selective generation of reactive oxygen species in cervical cancer cells, Mol. Carcino. 55 (2016) 918–928.

[48] M.A. Khan, S. Gahlot, S. Majumdar, Oxidative stress induced by curcumin promotes the death of cutaneous T-cell lymphoma (HuT-78) by disrupting the function of several molecular targets, Mol. Cancer Ther. 11 (2012) 1873–1883.

[49] J. Kang, J. Chen, Y. Shi, J. Jia, Y. Zhang, Curcumin-induced histone hypoacetylation: the role of reactive oxygen species, Biochem. Pharmacol. 69 (2005) 1205–1213.

[50] T. Rodrigues, A.C. Santos, A.A. Pigoso, F.E. Mingatto, S.A. Uyemura, C. Curti, Thioridazine interacts with the membrane of mitochondria acquiring antioxidant activity toward apoptosis–potentially implicated mechanisms, Br. J. Pharmacol. 136 (2002) 136–142.

[51] L. Serrander, L. Cartier, K. Bedard, B. Banfi, B. Lardy, O. Plastre, A. Sienkiewicz, L. Forro, W. Schlegel, K.H. Krause, NOX4 activity is determined by mRNA levels and reveals a unique pattern of ROS generation, Biochem. J. 406 (2007) 105–114.

[52] B.S. Chakraborty, K.K. Midha, G. McKay, E.M. Hawes, J.W. Hubbard, E.D. Korchinski, M.G. Choc, W.T. Robinson, Single dose kinetics of thioridazine and its two psychoactive metabolites in healthy humans: a dose proportionality study, J. Pharm. Sci. 78 (1989) 796–801.

[53] N.A. Buckley, I.M. Whyte, A.H. Dawson, Cardiotoxicity more common in thioridazine overdose than with other neuroleptics, J. Toxicol. Clin. Toxicol. 33 (1995) 199–204.

[54] S. Dallaire, Thioridazine (Mellaril) and mesoridazine (Serentil): prolongation of the QTc interval, CMAJ 164 (91) (2001) 95–99.

[55] J.T. Milnes, H.J. Witchel, J.L. Leaney, D.J. Leishman, J.C. Hancox, hERG K+ channel blockade by the antipsychotic drug thioridazine: an obligatory role for the S6 helix residue F656, Biochem. Biophys. Res. Commun. 351 (2006) 273–280.

[56] T. Seredenina, G. Chiriano, A. Filippova, Z. Nayernia, Z. Mahiout, L. Fioraso-Cartier, O. Plastre, L. Scapozza, K.H. Krause, V. Jaquet, A subset of N-substituted phenothiazines inhibits NADPH oxidases, Free Radic. Biol. Med 86 (2015) 239–249.

[57] T. Traykov, V. Hadjimitova, P. Goliysky, S. Ribarov, Effect of phenothiazines on activated macrophage-induced luminol-dependent chemiluminescence, Gen. Physiol. Biophys. 16 (1997) 3–14.

[58] C.D. Lao, M.Tt Ruffin, D. Normolle, D.D. Heath, S.I. Murray, J.M. Bailey, M.E. Boggs, J. Crowell, C.L. Rock, D.E. Brenner, Dose escalation of a curcuminoid formulation, BMC Complement. Altern. Med. 6 (2006) 10–13.

[59] S. Perkins, R.D. Verschoyle, K. Hill, I. Parveen, M.D. Threadgill, R.A. Sharma, M.L. Williams, W.P. Steward, A.J. Gescher, Chemopreventive efficacy and pharmacokinetics of curcumin in the min/+ mouse, a model of familial adenomatous polyposis, Cancer Epidemiol. Biomark. Prev. 11 (2002) 535–540.

[60] A.N. Begum, M.R. Jones, G.P. Lim, T. Morihara, P. Kim, D.D. Heath, C.L. Rock, M.A. Pruitt, F. Yang, B. Hudspeth, S. Hu, K.F. Faull, B. Teter, G.M. Cole, S.A. Frautschy, Curcumin structure-function, bioavailability, and efficacy in models of neuroinflammation and Alzheimer's disease, J. Pharmacol. Exp. Ther. 326 (2008) 196–208.

[61] S.S. Chiu, E. Lui, M. Majeed, J.K. Vishwanatha, A.P. Ranjan, A. Maitra, D. Pramanik, J.A. Smith, L. Helson, Differential distribution of intravenous curcumin formulations in the rat brain, Anticancer Res. 31 (2011) 907–911.

[62] K.I. Priyadarsini, The chemistry of curcumin: from extraction to therapeutic agent, Molecules 19 (2014) 20091–20112.

[63] V. Ravindranath, N. Chandrasekhara, Absorption and tissue distribution of curcumin in rats, Toxicology 16 (1980) 259–265.

[64] M.H. Pan, T.M. Huang, J.K. Lin, Biotransformation of curcumin through reduction and glucuronidation in mice, Drug Metab. Dispos. 27 (1999) 486–494.

[65] X. Chen, F. Zhi, X. Jia, X. Zhang, R. Ambardekar, Z. Meng, A.R. Paradkar, Y. Hu, Y. Yang, Enhanced brain targeting of curcumin by intranasal administration of a

thermosensitive poloxamer hydrogel, J. Pharm. Pharmacol. 65 (2013) 807–816.

[66] G. Shoba, D. Joy, T. Joseph, M. Majeed, R. Rajendran, P.S. Srinivas, Influence of piperine on the pharmacokinetics of curcumin in animals and human volunteers, Planta Med. 64 (1998) 353–356.

[67] C. Schiborr, A. Kocher, D. Behnam, J. Jandasek, S. Toelstede, J. Frank, The oral bioavailability of curcumin from micronized powder and liquid micelles is significantly increased in healthy humans and differs between sexes, Mol. Nutr. Food Res. 58 (2014) 516–527.

[68] K.M. Nelson, J.L. Dahlin, J. Bisson, J. Graham, G.F. Pauli, M.A. Walters, The essential medicinal chemistry of curcumin, J. Med. Chem. 60 (2017) 1620–1637.

[69] B.R. Seo, K.J. Min, S.M. Woo, M. Choe, K.S. Choi, Y.K. Lee, G. Yoon, T.K. Kwon, Inhibition of cathepsin S induces mitochondrial ROS that sensitizes TRAIL-mediated apoptosis through p53-mediated downregulation of Bcl-2 and c-FLIP, Antioxid. Redox Signal. 27 (2017) 215–233.

[70] R.P. Wilkie-Grantham, S. Matsuzawa, J.C. Reed, Novel phosphorylation and ubi-quitination sites regulate reactive oxygen species-dependent degradation of anti-apoptotic c-FLIP protein, J. Biol. Chem. 288 (2013) 12777–12790.

[71] P. Chanvorachote, U. Nimmannit, L. Wang, C. Stehlik, B. Lu, N. Azad, Y. Rojanasakul, Nitric oxide negatively regulates Fas CD95-induced apoptosis

through inhibition of ubiquitin-proteasome-mediated degradation of FLICE in-hibitory protein, J. Biol. Chem. 280 (2005) 42044–42050.

[72] A.M. Domina, J.A. Vrana, M.A. Gregory, S.R. Hann, R.W. Craig, MCL1 is phos-phorylated in the PEST region and stabilized upon ERK activation in viable cells, and at additional sites with cytotoxic okadaic acid or taxol, Oncogene 23 (2004) 5301–5315.

[73] Q. Ding, L. Huo, J.Y. Yang, W. Xia, Y. Wei, Y. Liao, C.J. Chang, Y. Yang, C.C. Lai, D.F. Lee, C.J. Yen, Y.J. Chen, J.M. Hsu, H.P. Kuo, C.Y. Lin, F.J. Tsai, L.Y. Li, C.H. Tsai, M.C. Hung, Down-regulation of myeloid cell leukemia-1 through in-hibiting Erk/Pin 1 pathway by sorafenib facilitates chemosensitization in breast cancer, Cancer Res. 68 (2008) 6109–6117.

[74] S.K. Nifoussi, J.A. Vrana, A.M. Domina, A. De Biasio, J. Gui, M.A. Gregory, S.R. Hann, R.W. Craig, Thr 163 phosphorylation causes Mcl-1 stabilization when degradation is independent of the adjacent GSK3-targeted phosphodegron, pro-moting drug resistance in cancer, PLoS One 7 (2012) e47060–e47073.

[75] Q. Ding, X. He, J.M. Hsu, W. Xia, C.T. Chen, L.Y. Li, D.F. Lee, J.C. Liu, Q. Zhong, X. Wang, M.C. Hung, Degradation of Mcl-1 by beta-TrCP mediates glycogen syn-thase kinase 3-induced tumor suppression and chemosensitization, Mol. Cell. Biol. 27 (2007) 4006–4017.